

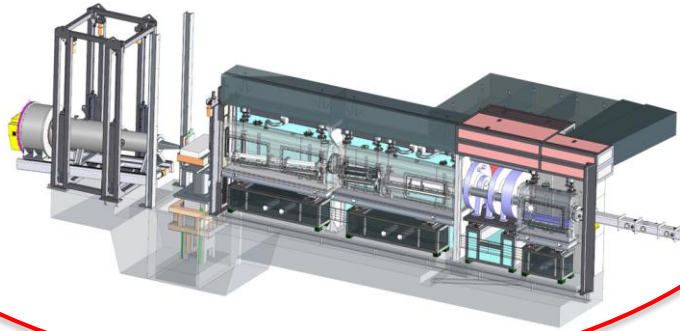
Liquid Surface Scattering at ILL

[Philipp Gutfreund](#)

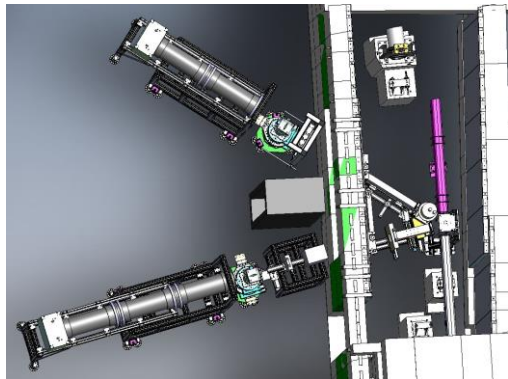
ILL, Grenoble, France

Liquid Surface Scattering machines at ILL

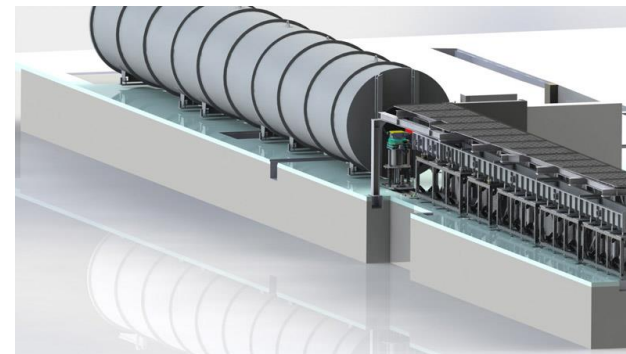
FIGARO
(horizontal reflectometer):

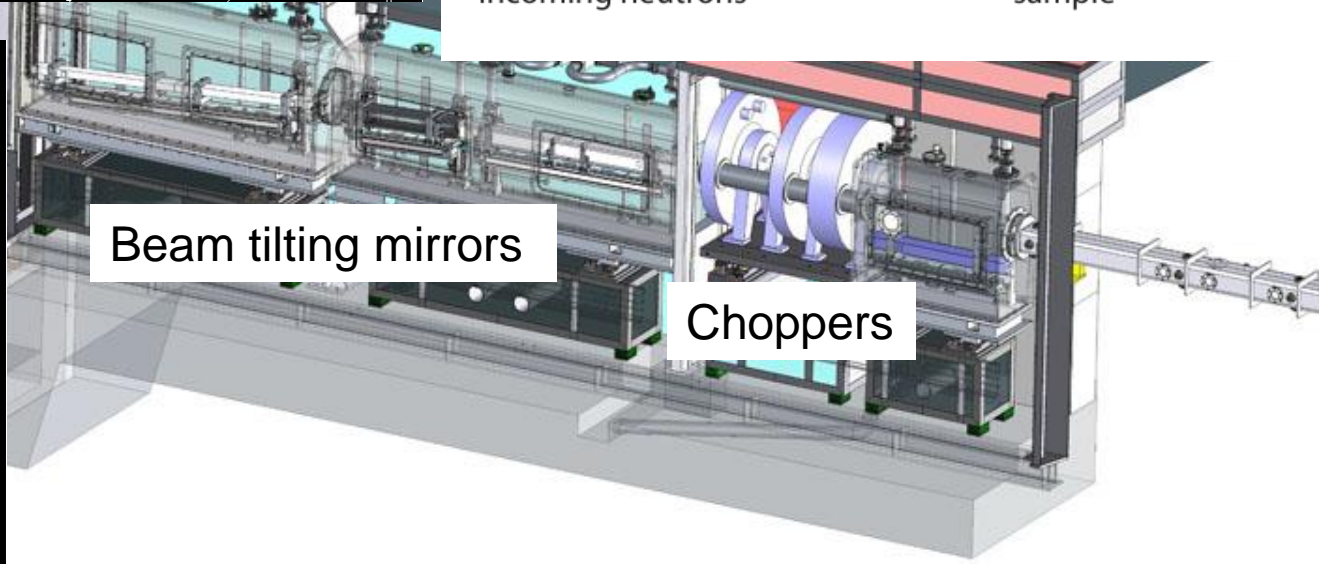
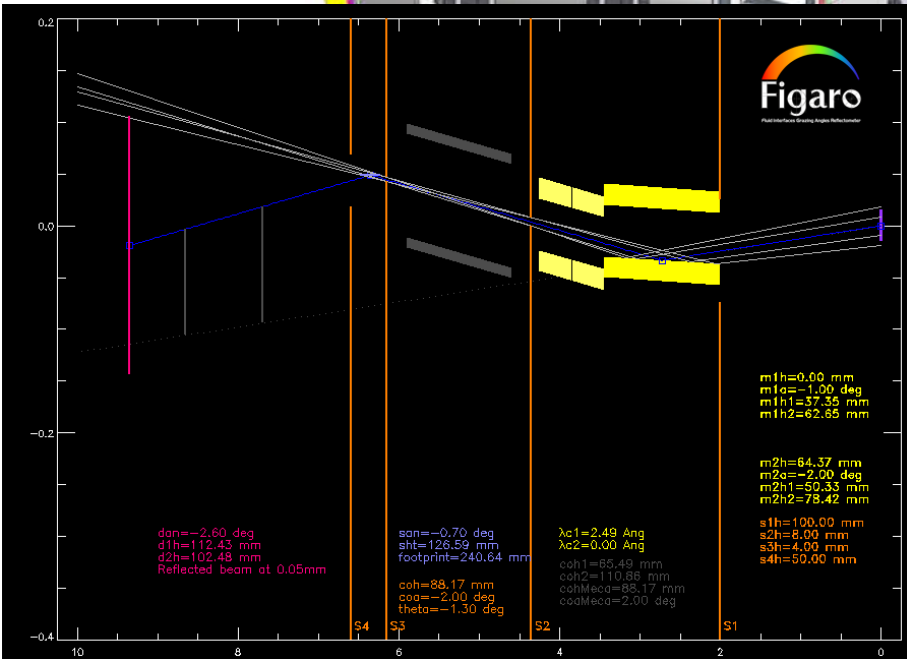
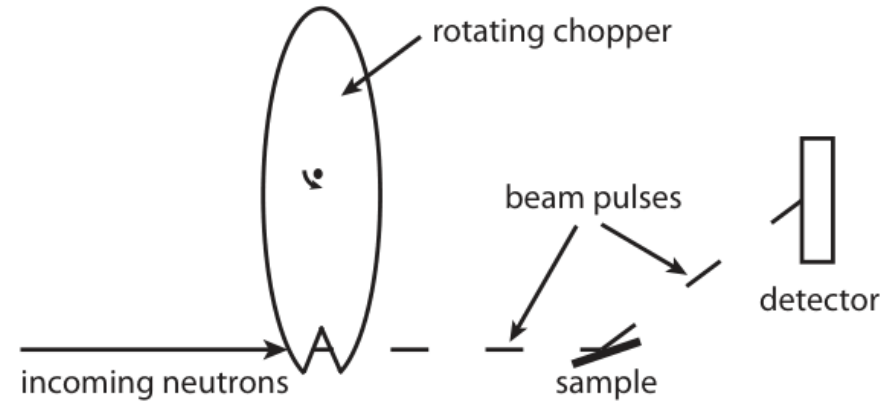
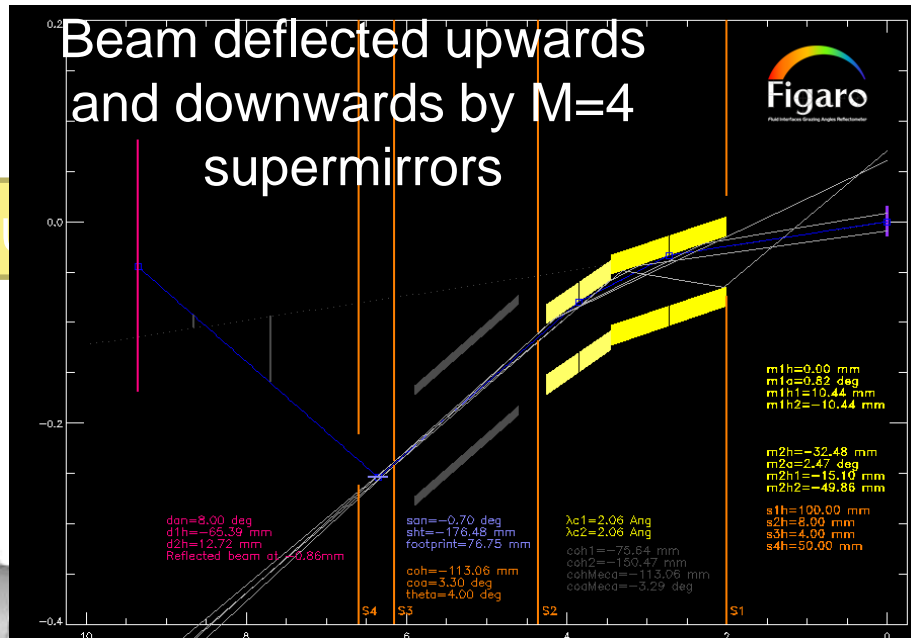


Super-ADAM
(vertical monochromatic Reflectometer
with horizontal Pseudo-GISANS option):



D22
(SANS machine
with GISANS option):





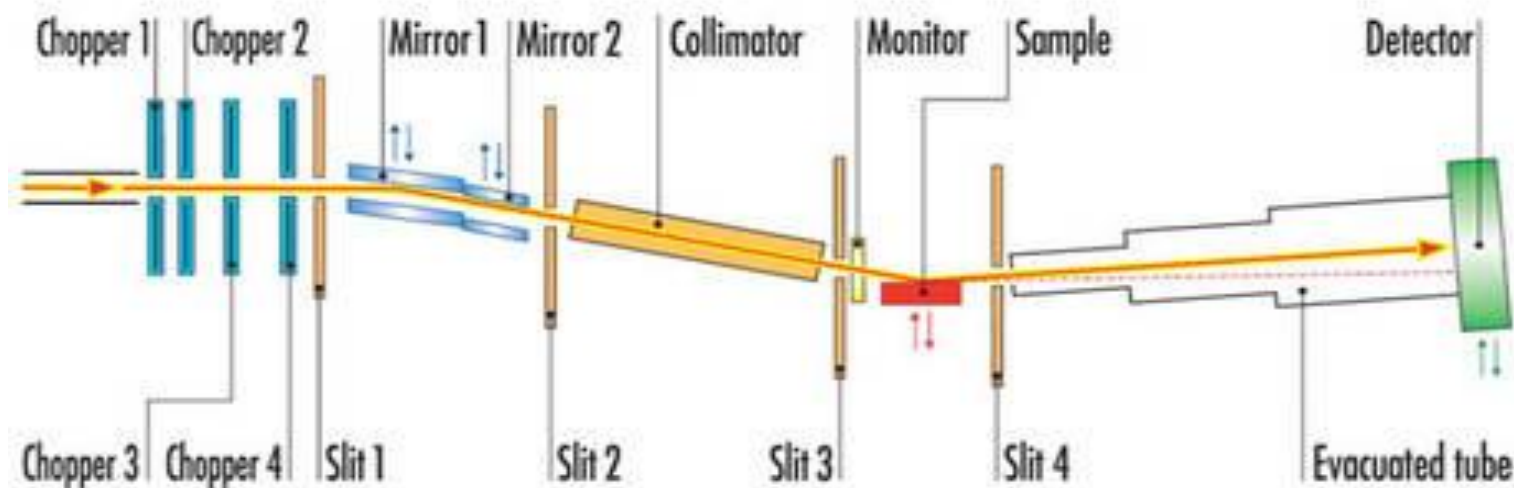
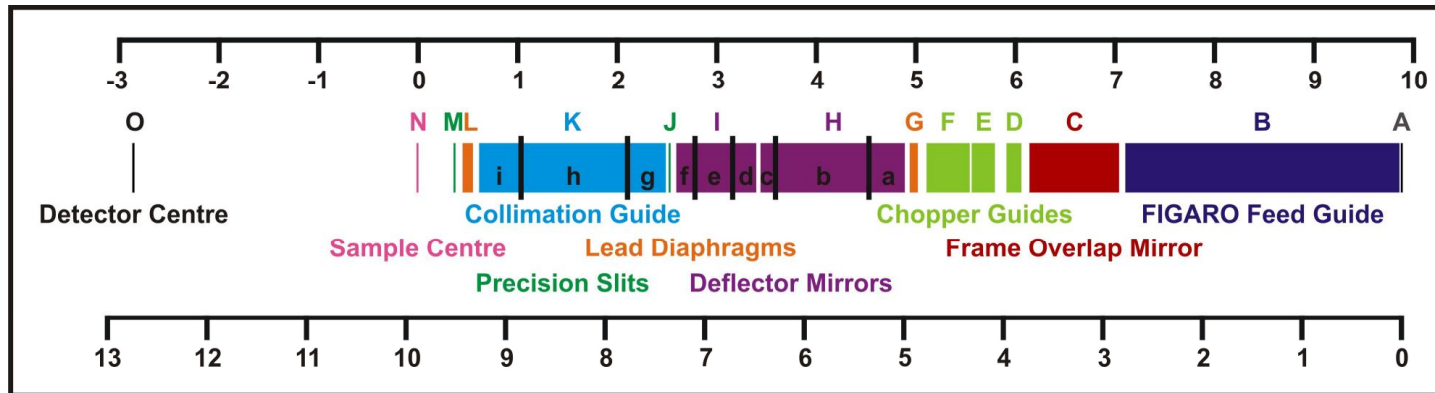
Campbell, R. *et al.* Eur. Phys. J. Plus, (2011) 126, 107.

Beam strikes both sides of interfaces

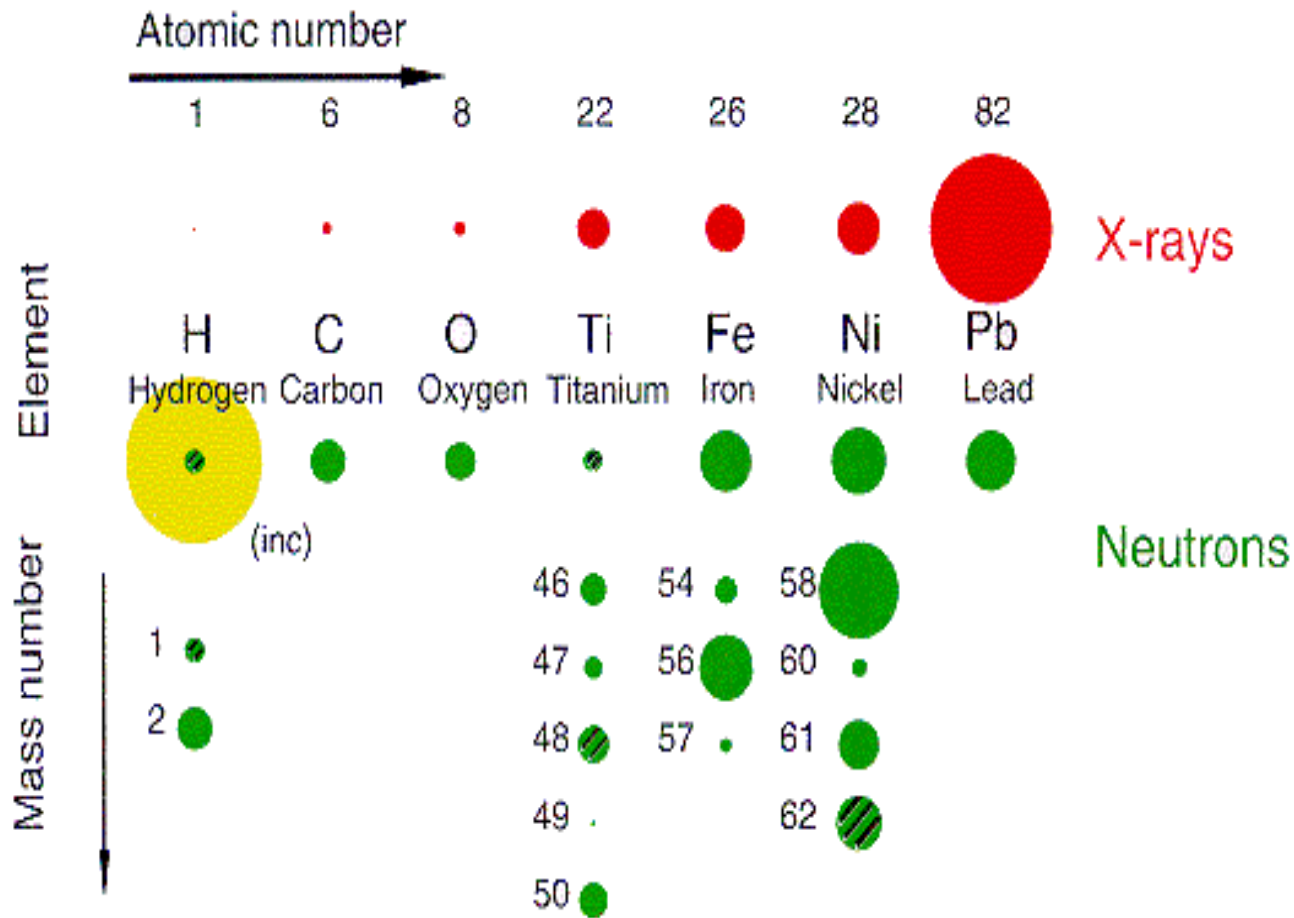
FIGARO

Typical incoming beam divergence (5 m collimation) (v x h) FWHM:
 Detector resolution at 2.8 m (v x h) FWHM:

0.005° - 0.1° x 0.05 - 0.1°
 0.045° x 0.09°



Scattering cross sections for neutrons and X-rays



The diameters of the circles shown scale with the scattering amplitude f_x ($\sin\theta=0$) for x-rays, and $b_{coh} \cdot 10$ for neutrons. Hatching indicates negative scattering amplitudes.

- Origins of scattering differ for the different methods.
- **X-rays** dominated by number of **electrons**.
- **Neutrons** rely on contrast of **nucleus**: similar for many different elements, but show **strong variations from different isotopes of same element, especially hydrogen**.
- **Absorption** cross-section **orders of magnitude lower** than scattering cross-section **for neutrons** in most materials.

Applications of Neutron Reflectometry

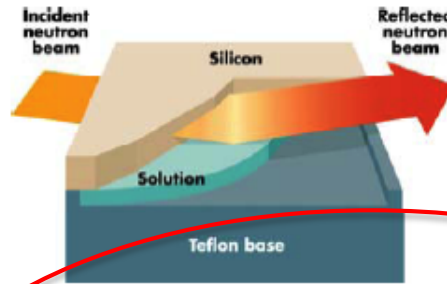
Kinetics

- Polymer Diffusion
- Critical exponents in SCF
- Protein unfolding
- Non equilibrium surfactant films
- Temporal resolution of

- Ion transfers
- Solvent transfers
- Polymer structure

Electrochemistry

- Electrodeposition and Surface nucleation
- Self Assembly of systems
 - Metal Hydroxide electroprecipitation (batteries)
 - Novel templating mechanisms

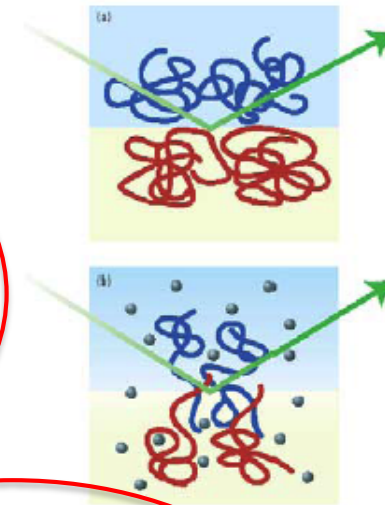
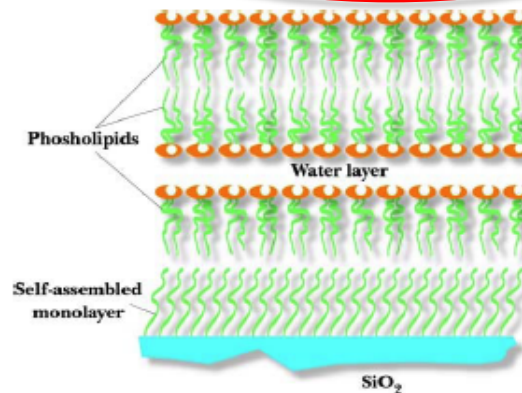


Model Devices

- Thin polymer films (finite size effects)
- Spin coating

Surfactants

- Parametric Studies
- Liquid/Liquid Interface
- Reduce Label size in Structural Studies
- Self Assembly
- Foams



Biology

- Protein adsorption
- Biocompatible polymers
- Drug transport
- Anaesthesia mechanisms

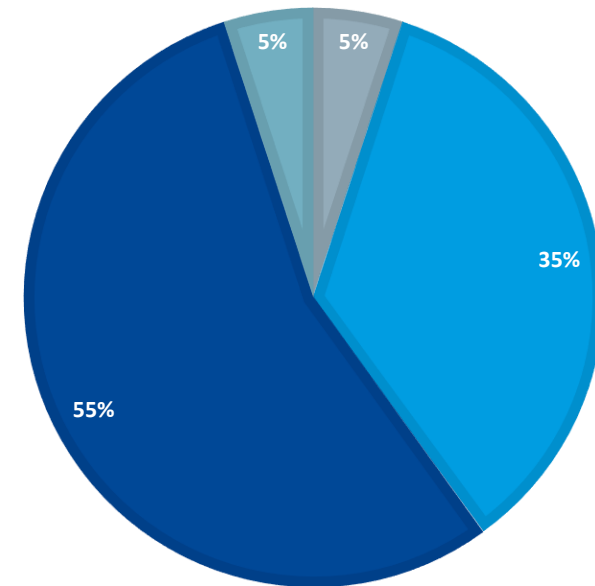
Magnetism:

- Magnetic multilayers
- Thin magnetic films
- Thin film magnetometry

SUMMARY OF SCIENTIFIC ACTIVITY

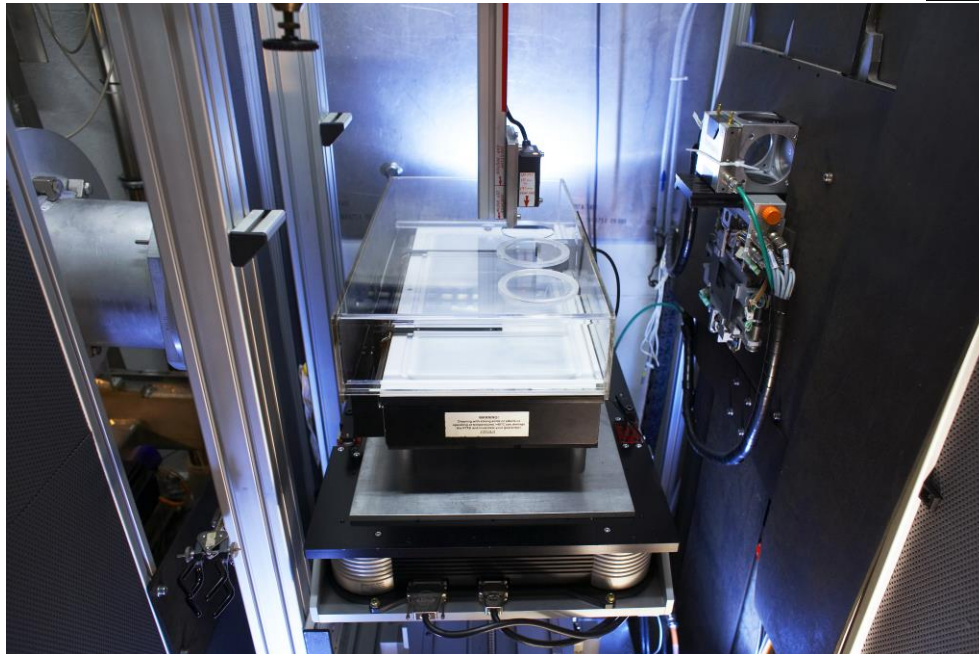
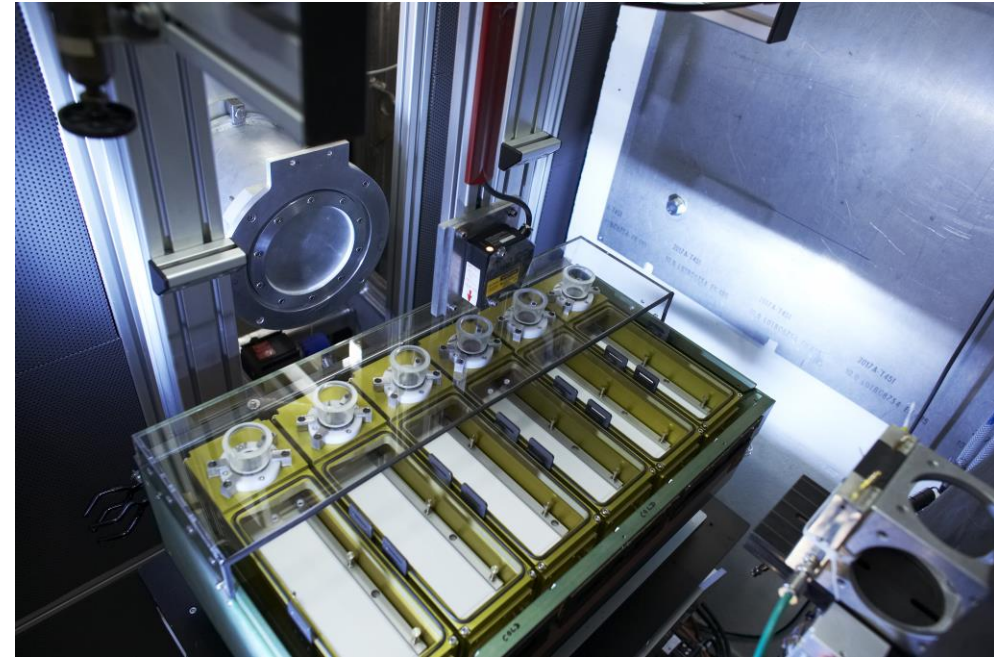
PUBLICATIONS 2023

■ Crystallography + Chemistry ■ Biology ■ Soft Matter ■ Nuclear and Particle Physics

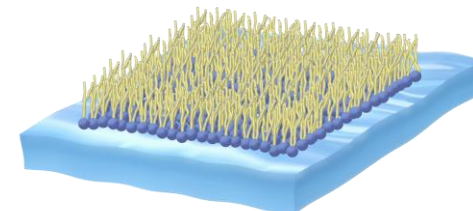


- Main scientific areas on FIGARO are Soft Matter and Biology.

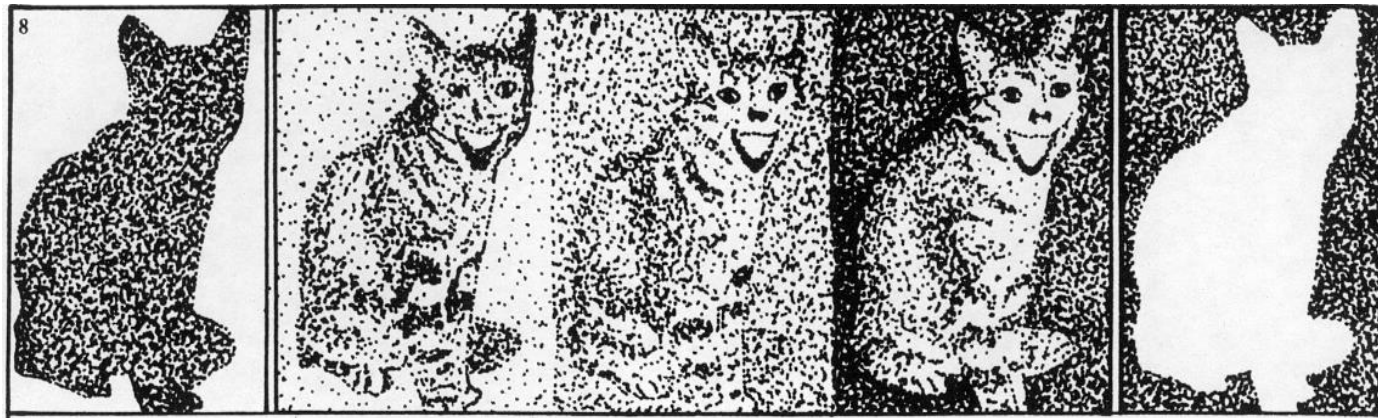
SAMPLE ENVIRONMENT



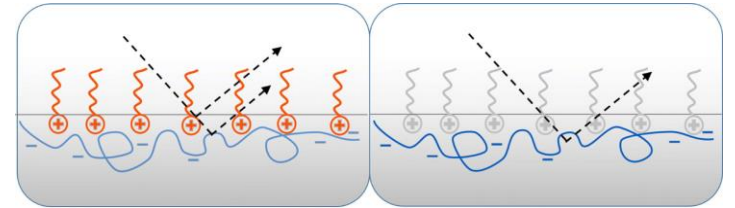
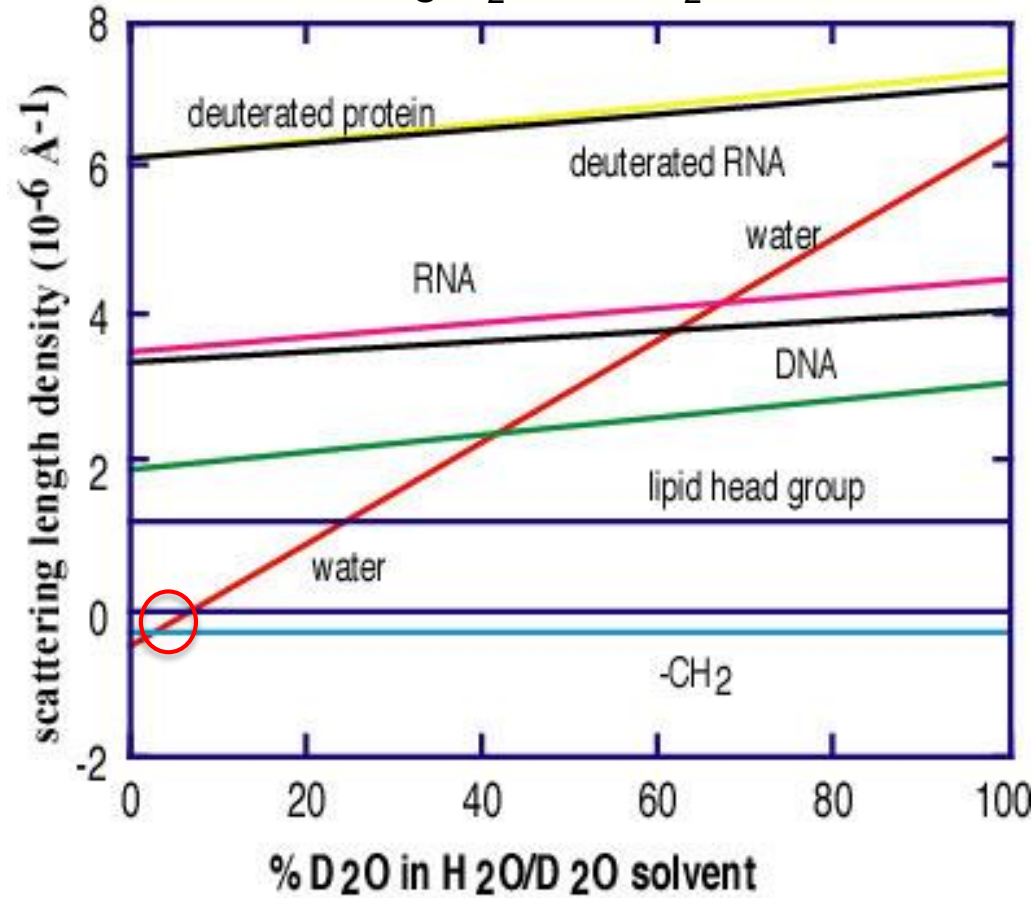
Langmuir trough for insoluble monolayers



Example I: Direct surface excess,
composition and structural measurements
by scattering contrast matching



Mixing D₂O and H₂O:



Braun et al., *Adv. Coll. Interf. Sci.* **247** (130-148) 2017

For: $q \cdot \sigma \ll 1$ and $q \cdot d \ll 1$

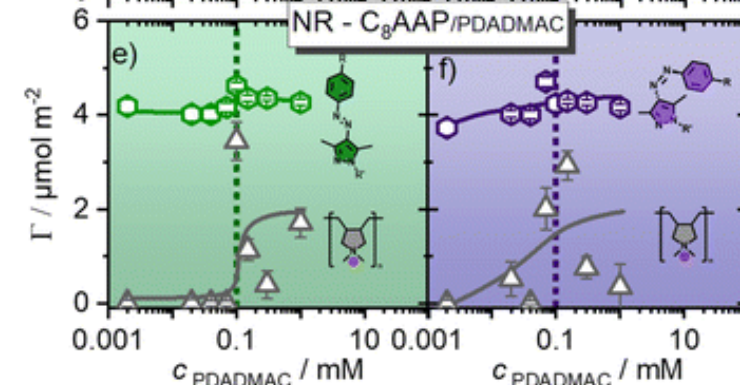
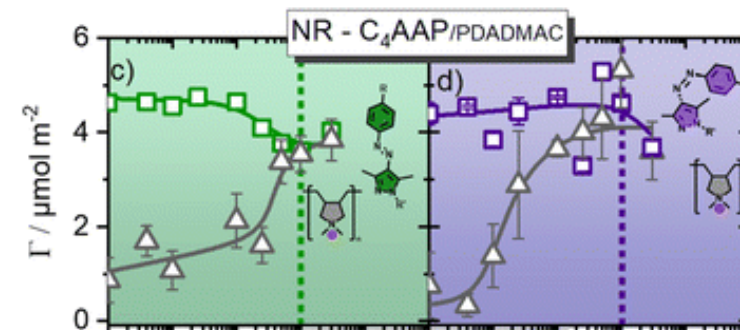
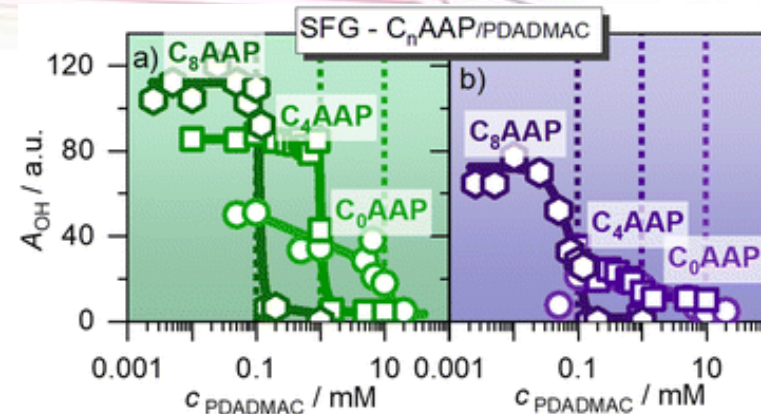
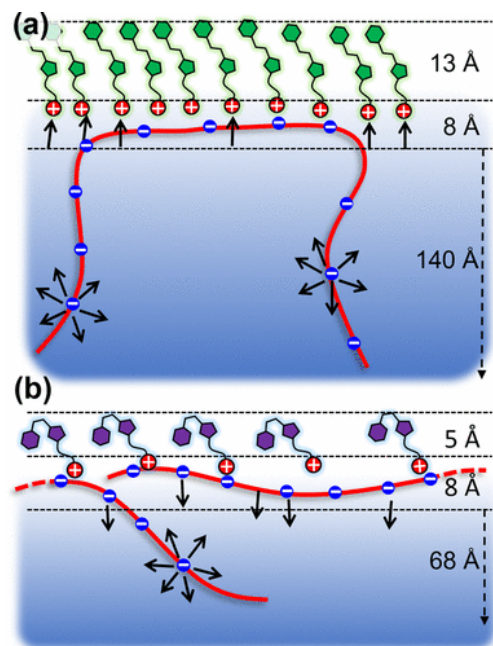
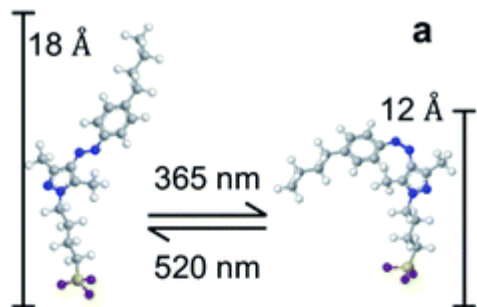
$$R \approx (4\pi/q)^2 (b \cdot \Gamma)^2$$

Zero-SLD-matched water

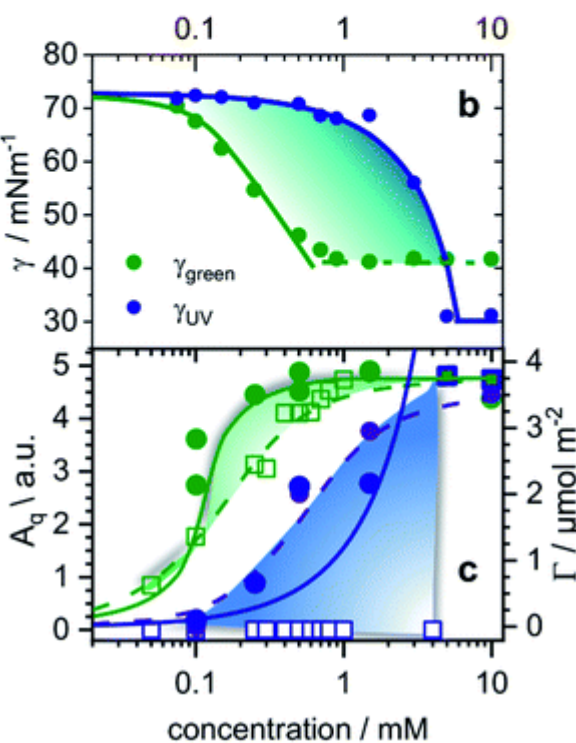
Example Ia: Polymer/Surfactant mixtures at the air-water interface

Photo-switchable surfactants and P/S mixtures

Individual kinetic surface excess and structure revealed by NR

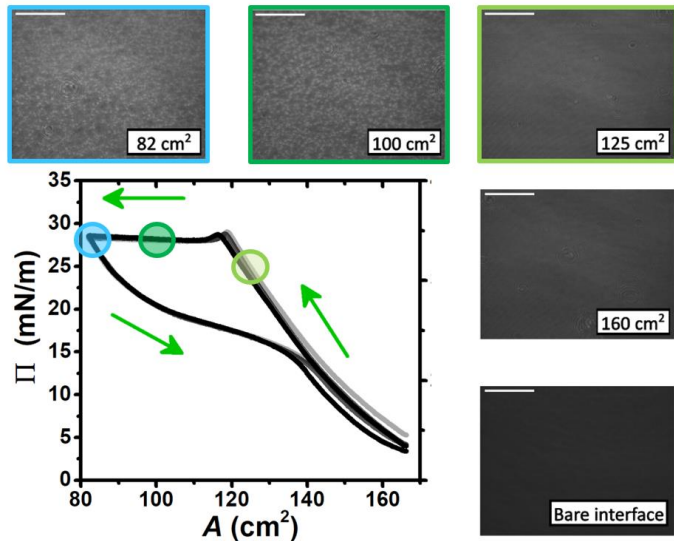
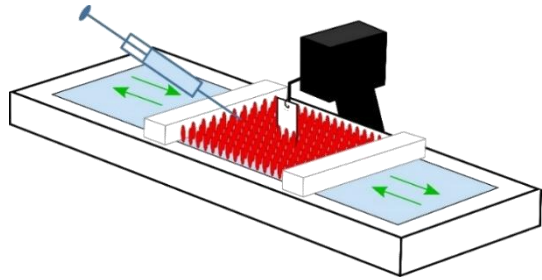


Honnigfort *et al.*, *Chem. Sci.* **11** 2085-2092 (2020)
 Schnurbus *et al.*, *J. Phys. Chem. B.* **124** 31 (2020)
 Schnurbus *et al.*, *ACS Appl. Mat. Interf.* **14** 3 (2022)
 Hardt *et al.*, *Langmuir* **39** 16 (2023)
 Hardt *et al.*, *Nanoscale* **16** 9975-9984 (2024)



3D CONTROL OF EXTENDED STRUCTURES IN POLYELECTROLYTE/SURFACTANT FILMS

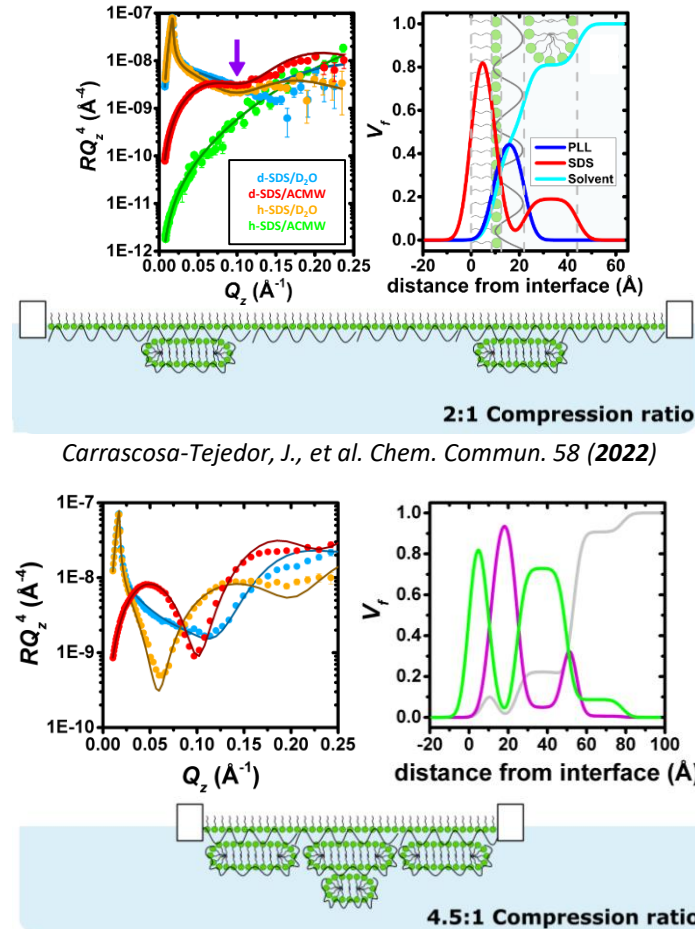
Spread P/S films at the air/water interface



- Monolayer's coverage control
- Switch on/off 3D extended structures
- 3D extended structures' coverage control

LINEAR POLYPEPTIDES

Structural control via **compression ratio**

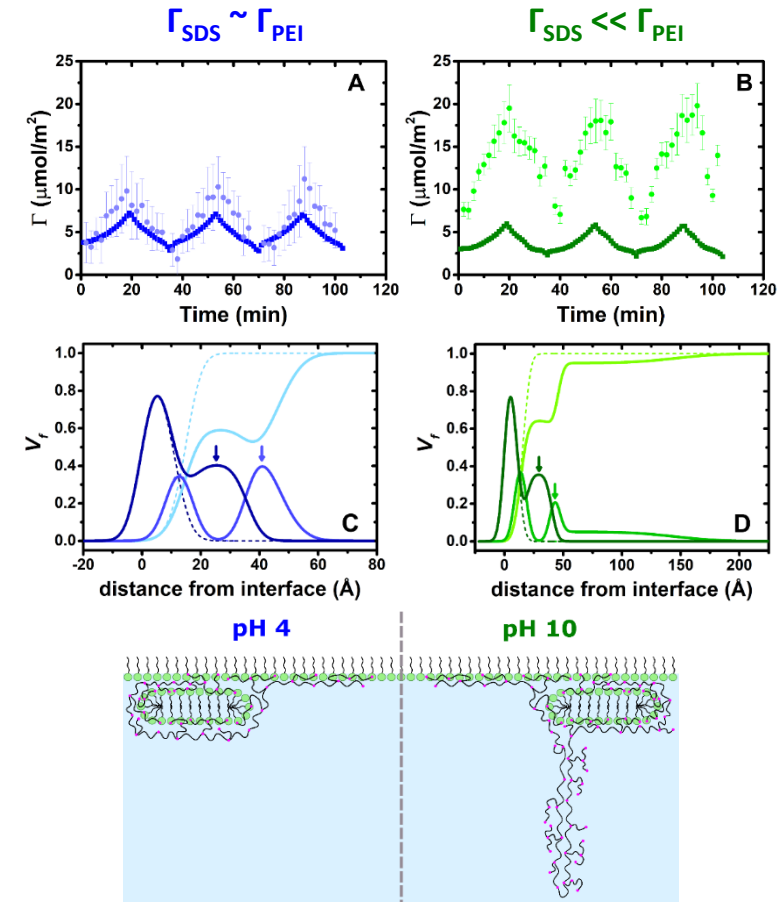


Carrascosa-Tejedor, J., et al. *Chem. Commun.* 58 (2022)

Carrascosa-Tejedor, J., et al. *Nanoscale* 15 (2023)

HYPERBRANCHED POLYELECTROLYTES

Structural control via **pH**

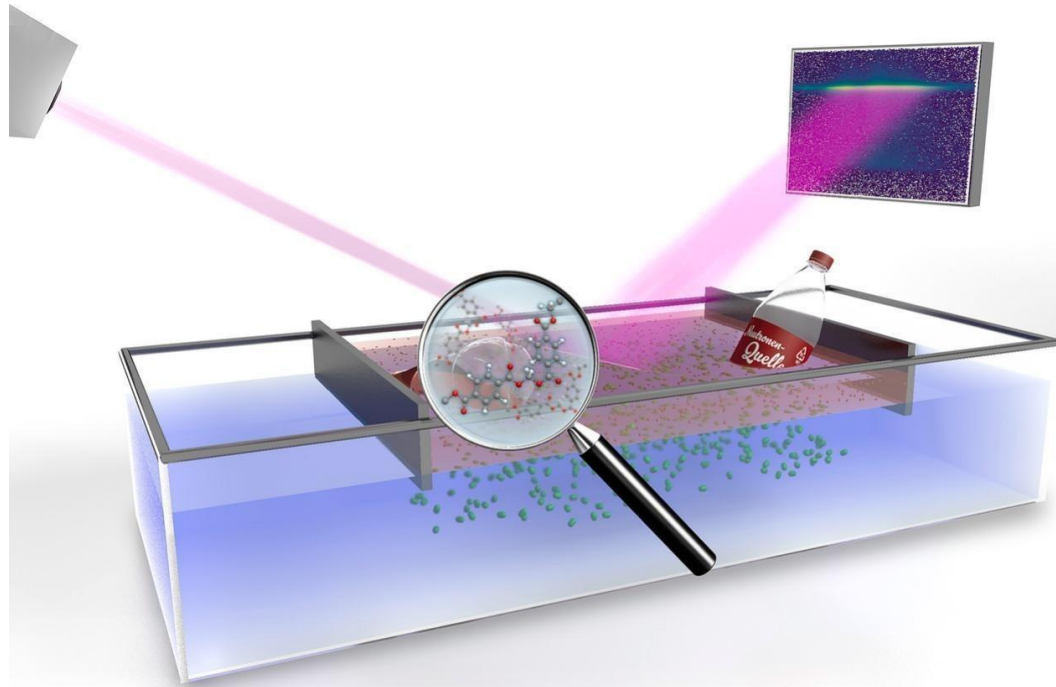


Carrascosa-Tejedor, J., et al. *Langmuir* 39 (2023)

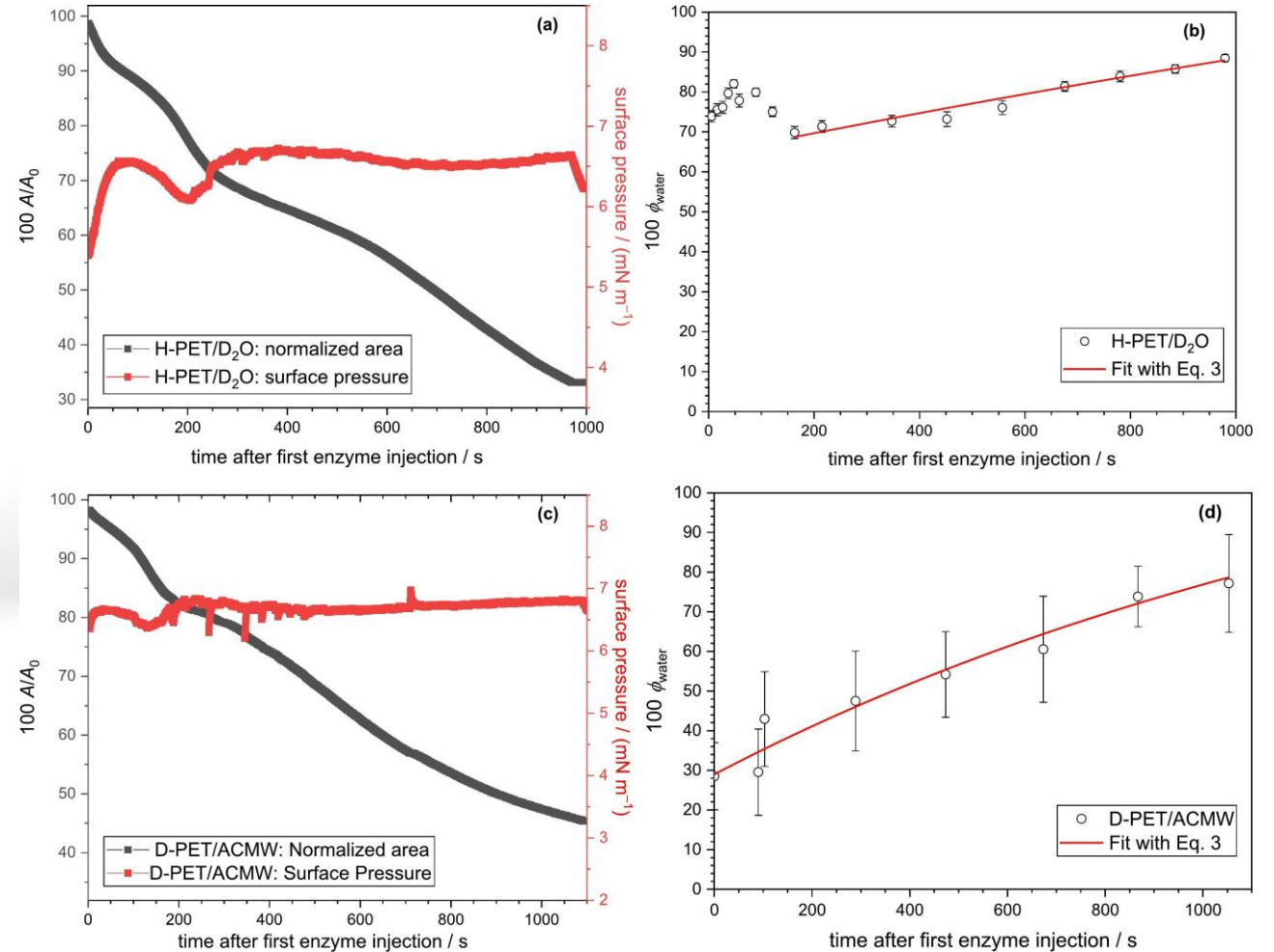
Example 1b: Enzyme activity at the air-water
and oil-water interface

enzymatic poly(ethylene terephthalate) hydrolysis

Kinetics of PET hydrolysis from NR



© Reiner Müller: FRM II / TUM

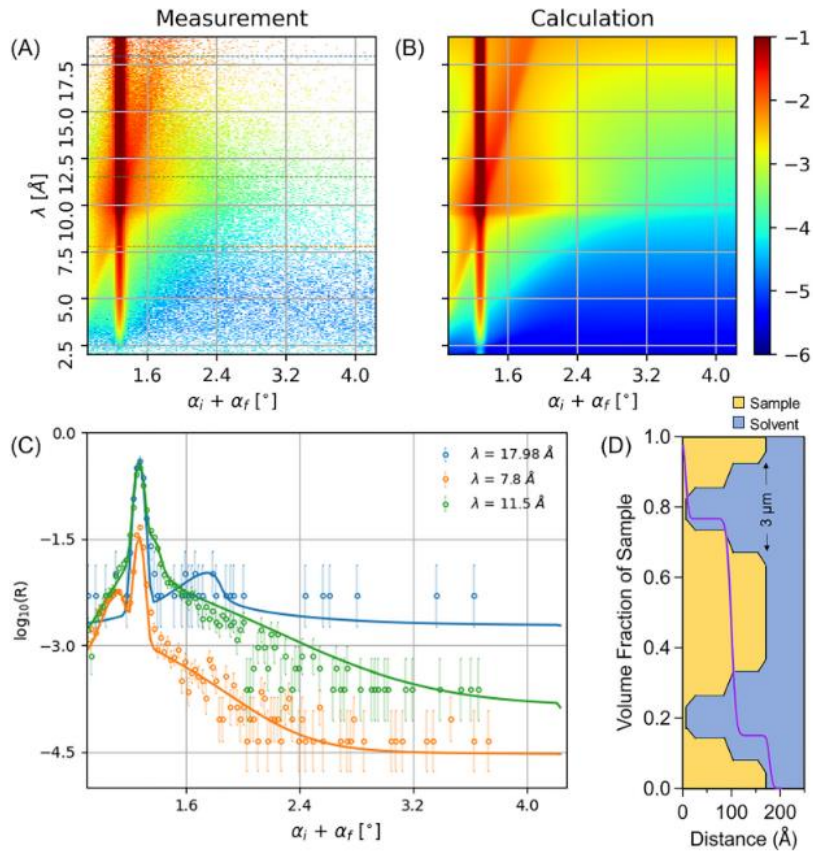


Machatschek et al., *J. Coll. Interf. Sci.* **698** 138021 (2025).

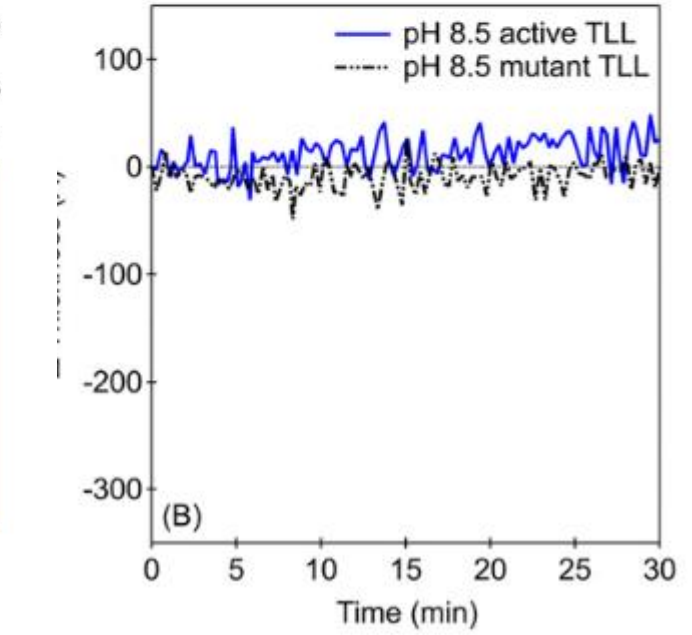
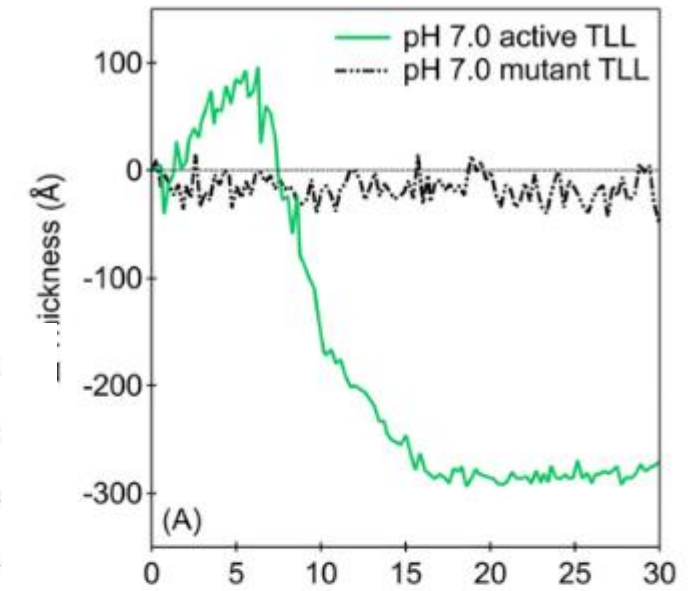
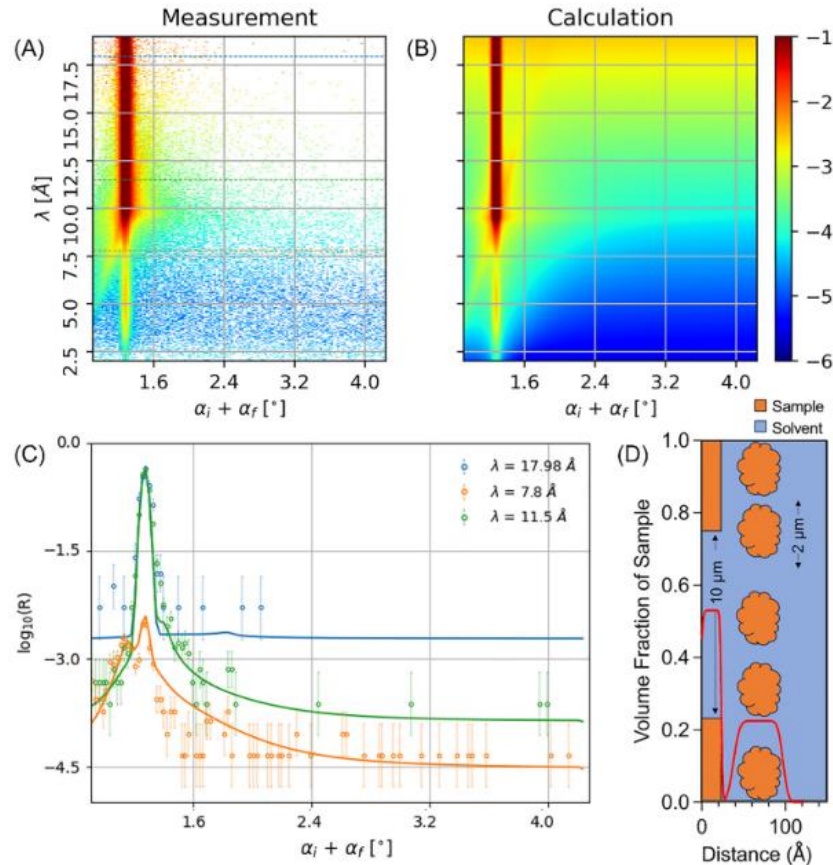
Structural changes of triolein films during lipolysis

Triolin oil digestion kinetics from NR
In-plane structure from OSS

Before digestion:



After digestion:

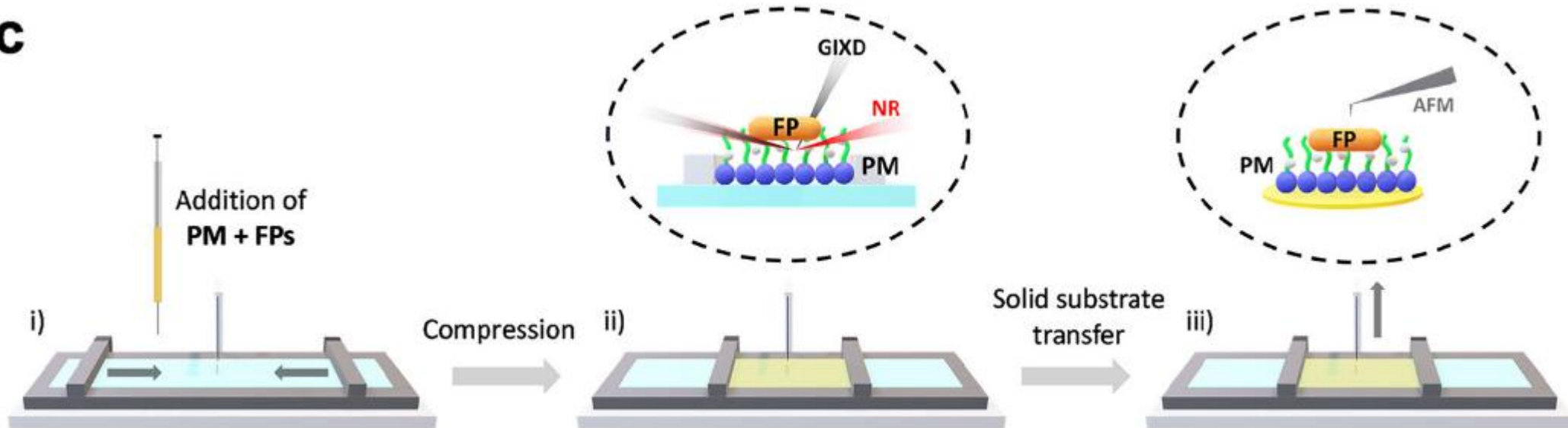


Example 1c: Protein/membrane interactions at the air-water interface

Interaction of sars-cov-2 fusion peptides with biomimetic plasma membranes

Monolayer composition extracted from contrast matching

C



Peptide assembly at the air/liquid interface

Structure/orientation of peptides

ADVANCED
SCIENCE NEWS

www.advancedsciencenews.com

ADVANCED
FUNCTIONAL
MATERIALS

www.afm-journal.de

Combination with
interfacial rheology:

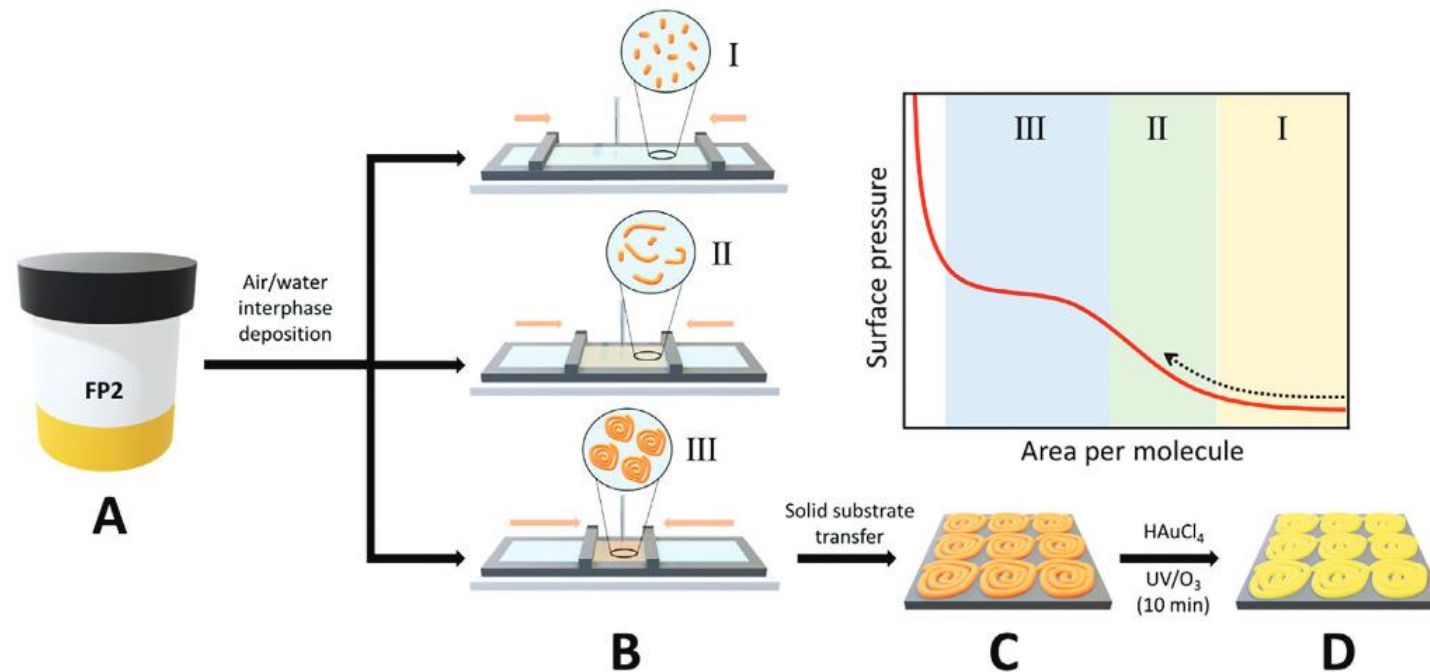


Figure 1. Schematic summary of the experimental approach. A) Preparation of the peptide solution into DMF. B) Deposition at the air–water interface and compression using a LB set-up. C) Transfer to mica substrate. D) Selective impregnation with metallic salt and peptide removal with UV/O_3 .

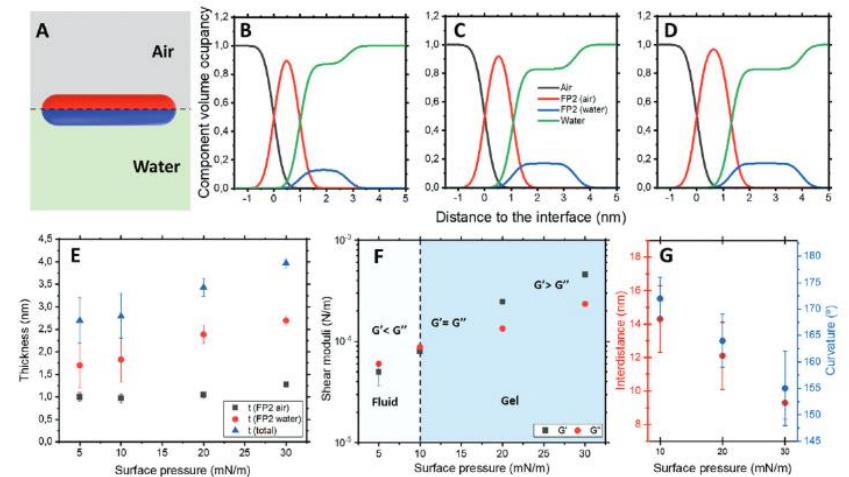
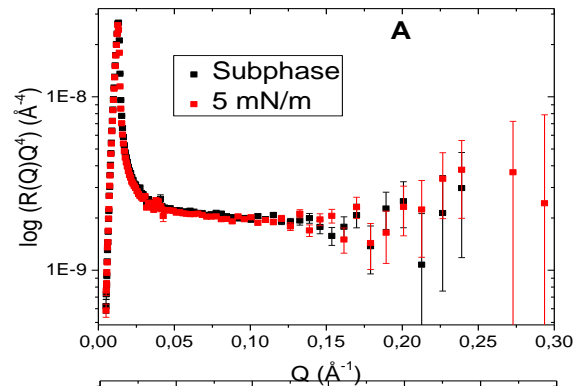


Figure 4. A) Schematic of the model used to fit NR data. Density profiles of the interfaces at B) 10, C) 20, and D) 30 mN m^{-1} . E) The total thickness of the fibers obtained by NR. F) Interfacial shear rheological measurements. G) Interdistance and curvature of the fibers were obtained by analysis of the AFM images.

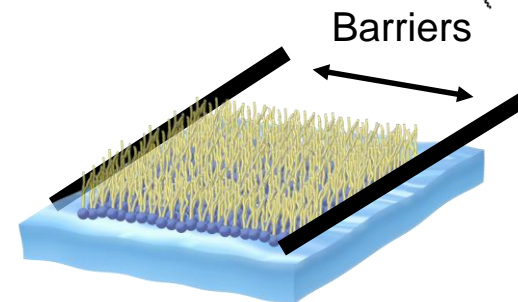
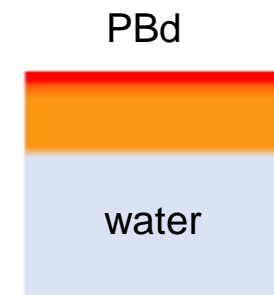
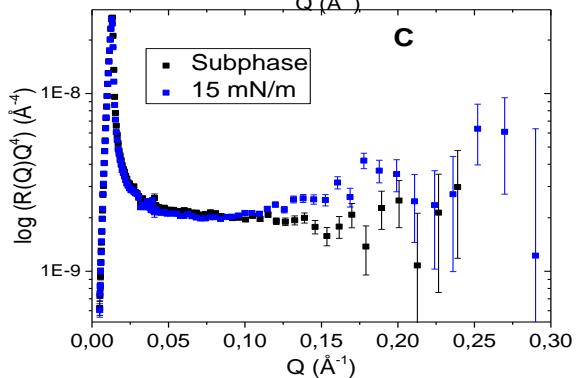
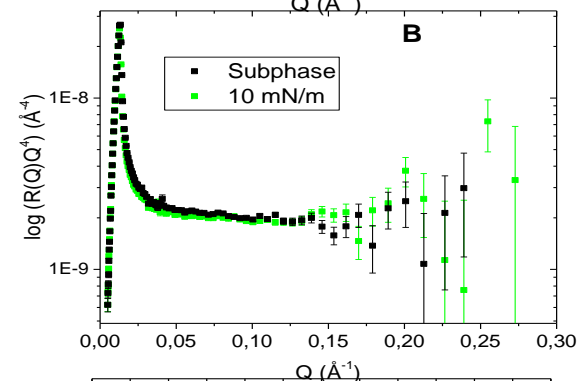
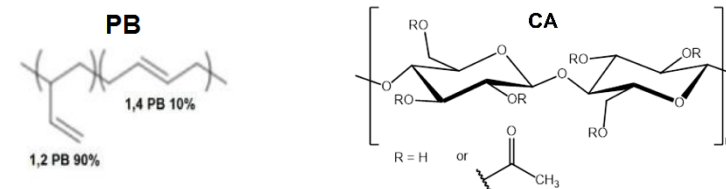
Example Id: Polymer blend phase separation at the air-water interface

Co-polymer Langmuir monolayers



Structure of hydrophobic (polybutadiene)/
hydrophilic (cellulose acetate) polymer blend
at the air/water interface.

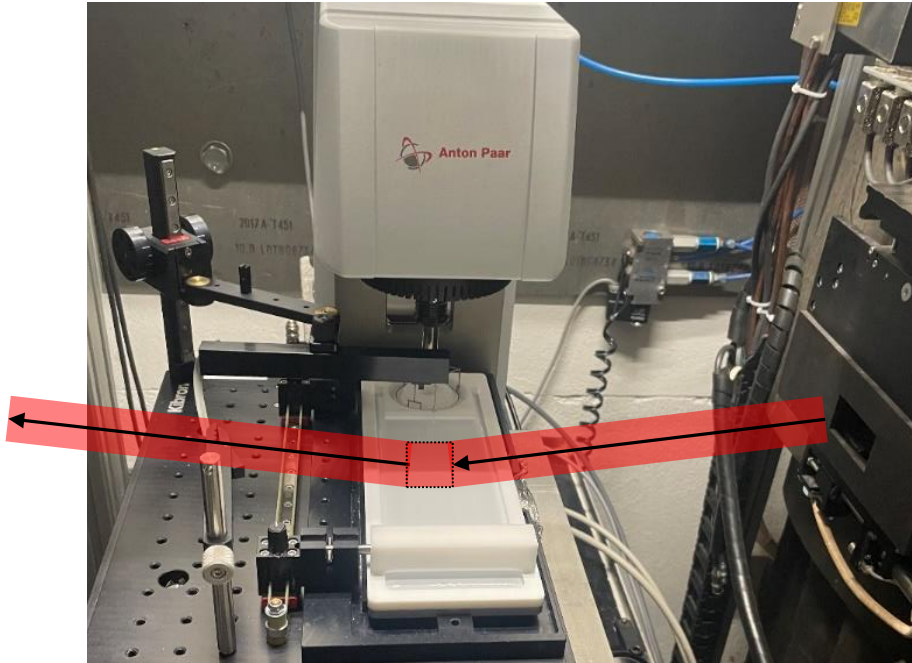
$$Nb_{PBd} = 5.72 \cdot 10^{-6} \text{ \AA}^{-2} \quad Nb_{CA} = 1.23 \cdot 10^{-6} \text{ \AA}^{-2}$$



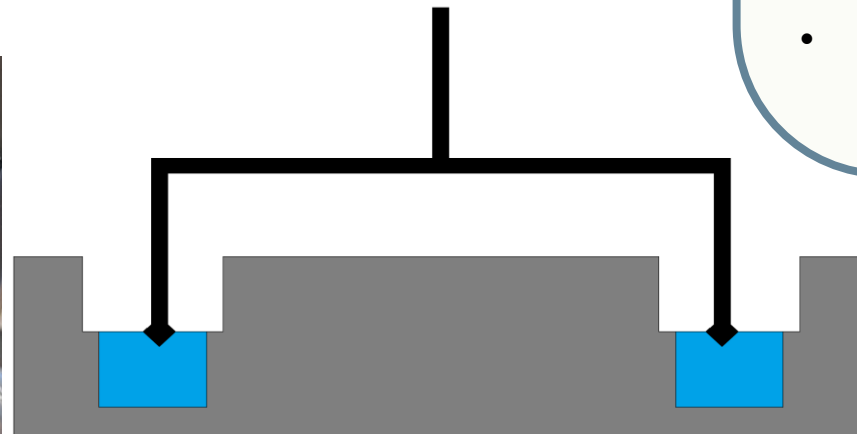
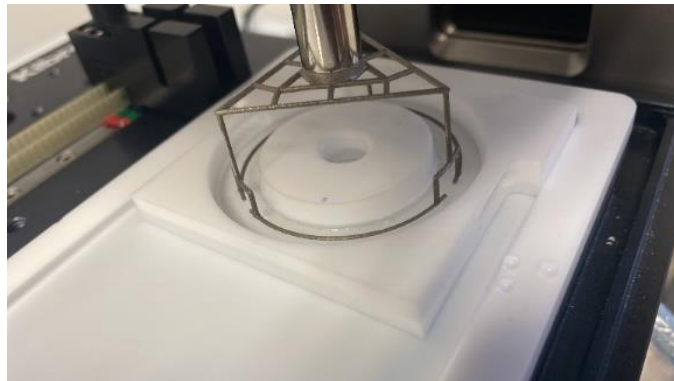
Water contrast-matched
to CA/BP mixture

Example II: Combination of NR and interfacial rheology

In situ interfacial rheology and Langmuir trough



Langmuir trough



Double-wall ring

Pros:

- High shear stresses.
- Large frequency range.
- Area in contact with bulk phases much smaller than in bicone.
- Large interfacial contact line.
- Small probe inertia.
- Measurement lower limit:
 $10^{-6} \text{ N/m} \leq G''_s$.

Drawback:

- Drive inertia limits frequency response.

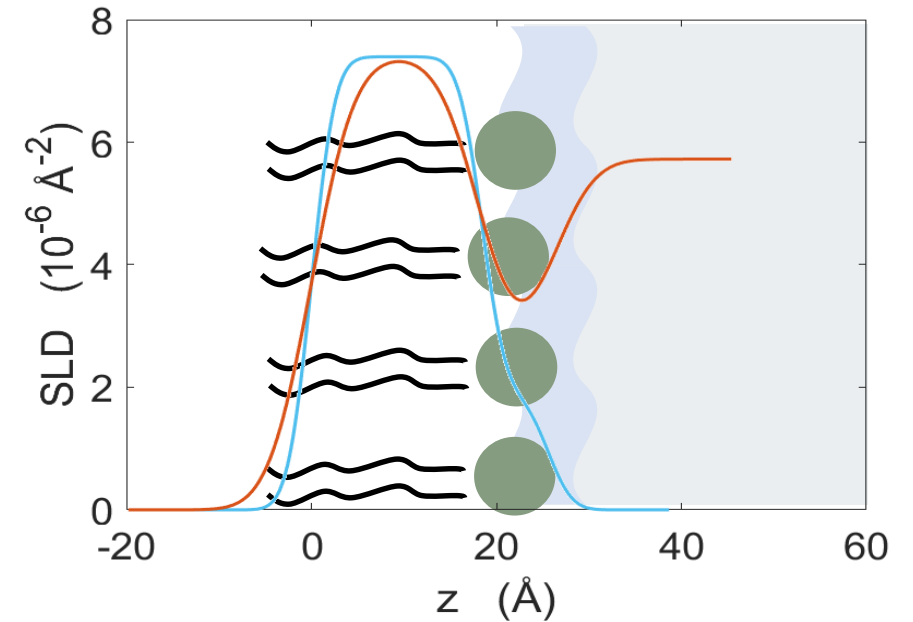
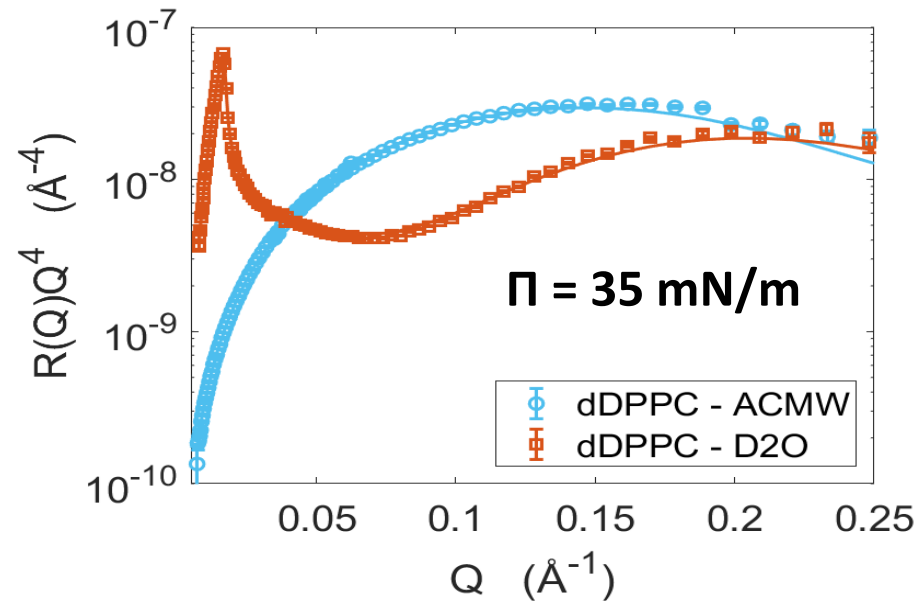
S. Vandebril et al, *Rheol. Acta* 49, 131-144, (2010)

B. Schroyen et al. *Rheol. Acta* 56, 1-10, (2017)

D. Renggli et al., *J. Rheol.* 64(141), (2020)

Double-wall ring set-up

DPPC – Structural analysis using NR



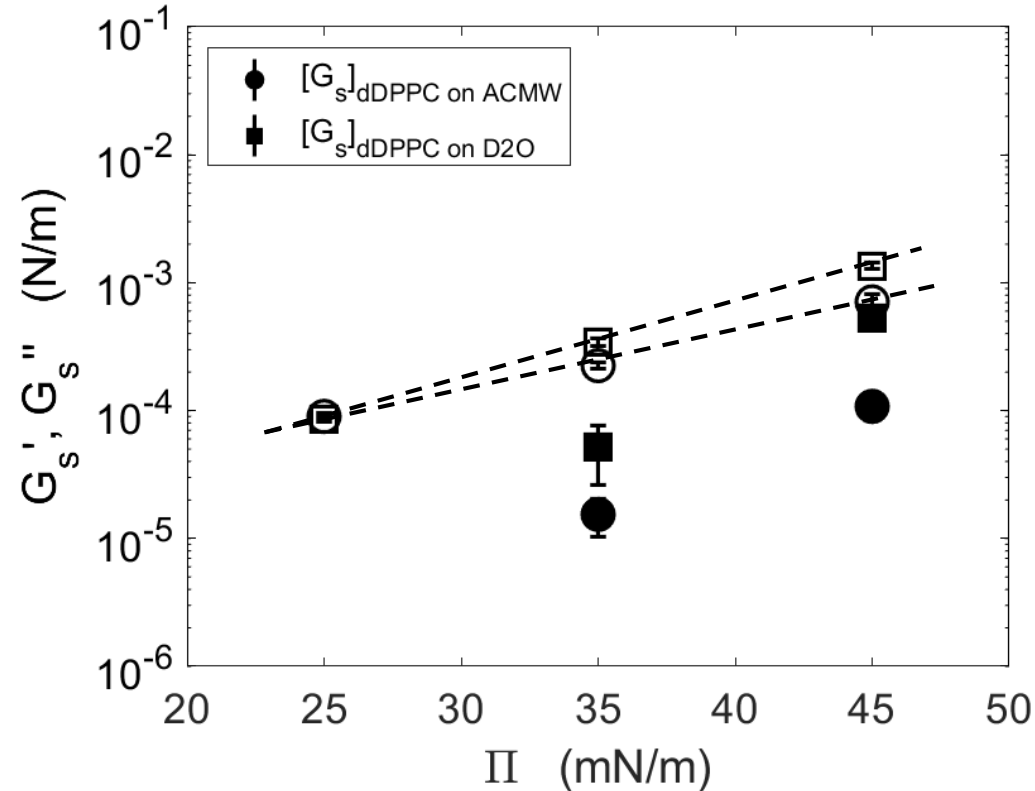
R. A. Campbell *JCIS* (2018)

Π (mN/m)	Chains thickness (\AA)	Headgroup thickness (\AA)	Area per molecule (\AA^2)
25	18.10	8	48.95
35	18.47	7.16	44.91
45	18.77	7.28	44.21

Double-wall ring set-up

DPPC - Rheology

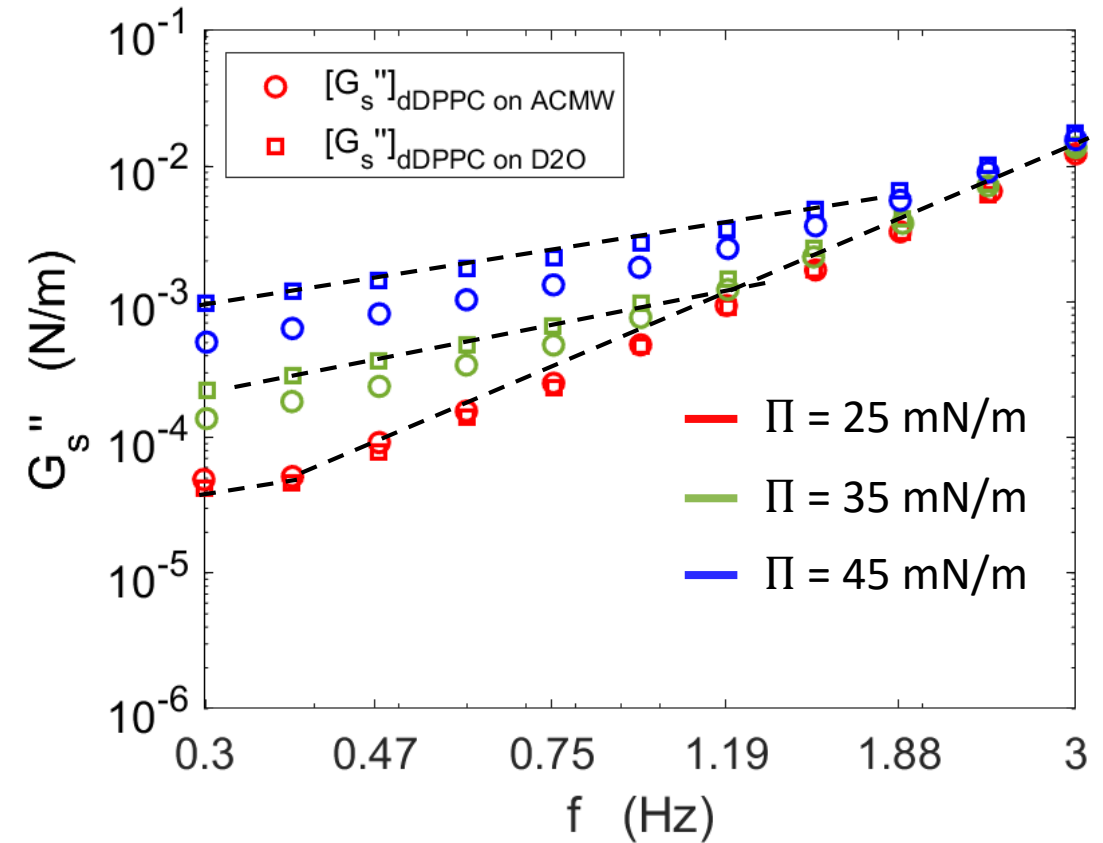
3% Strain, $f = 0.5$ Hz



G'_s → Filled symbols

G''_s → Open symbols

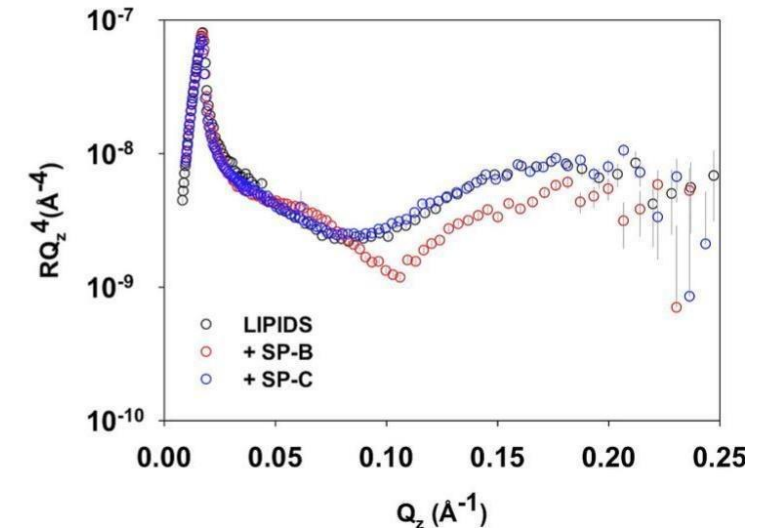
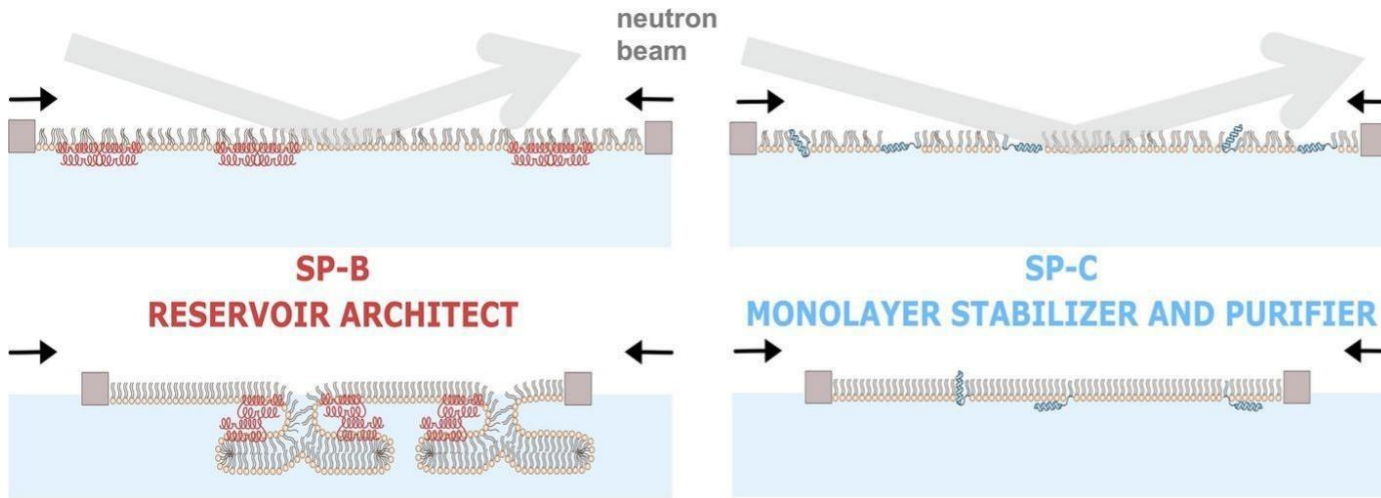
3% Strain, $f = 0.3 - 3$ Hz



E. Hermans *et al.* *Soft Matter* 2014

THE EUROPEAN NEUTRON SOURCE

Example IIb: Lung surfactant structure at the air-liquid interface



QT trough

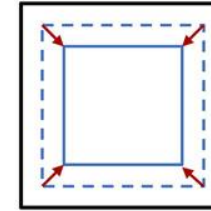
Quadrotrough: *In situ* Dilation or shear of Langmuir monolayers



(a)

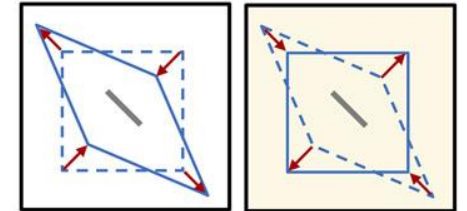
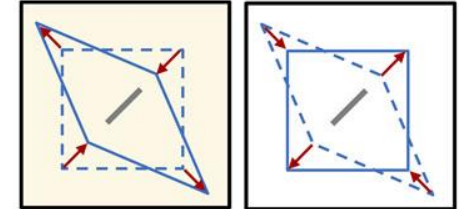
Quadrotrough Strain Modes

Dilation/Compression



Planar Shear Stretch

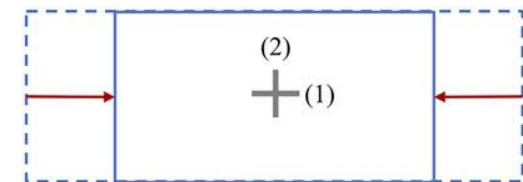
Shear Forward A (+ γ) Shear Backward A (- γ)



Shear Forward B (- γ) Shear Backward B (+ γ)

(b)

Langmuir Trough Mixed Flow



Tein *et al.* Rev. Sci. Instrum.. 2022;93(9).

ETH zürich

Jan Vermant

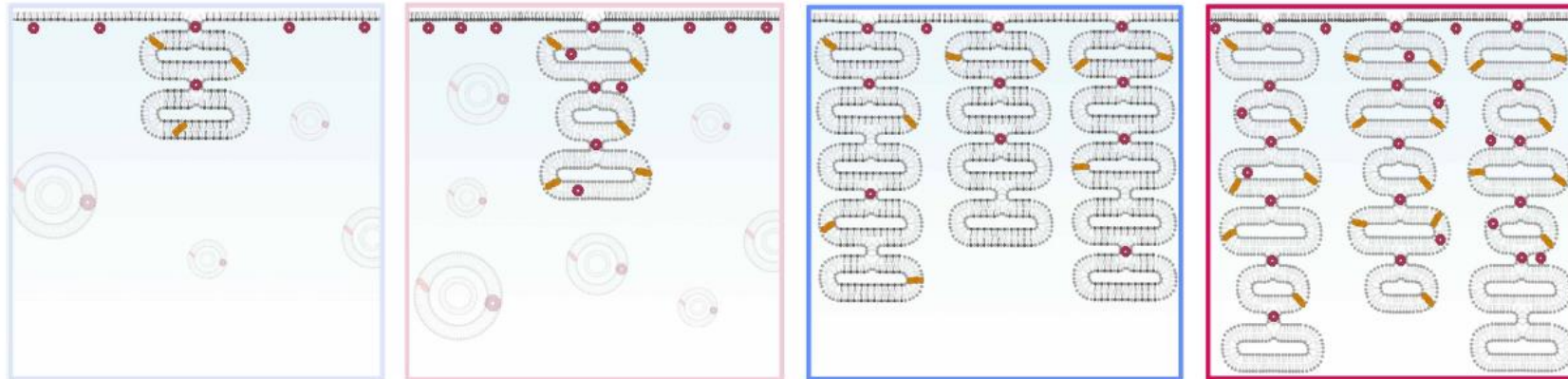
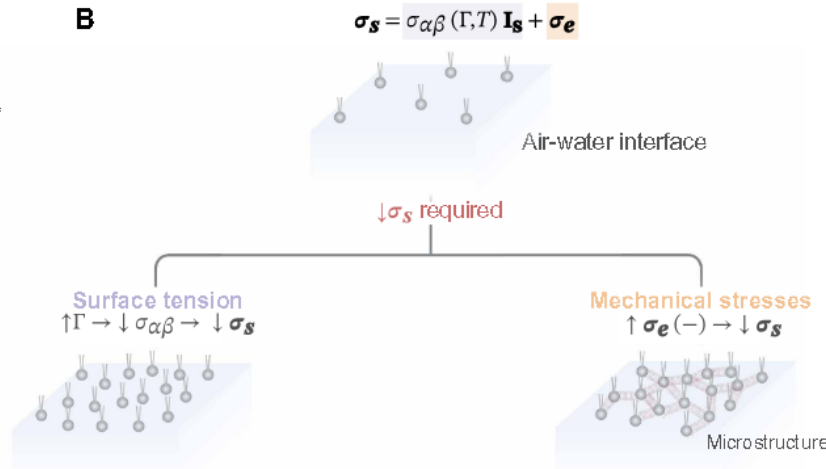
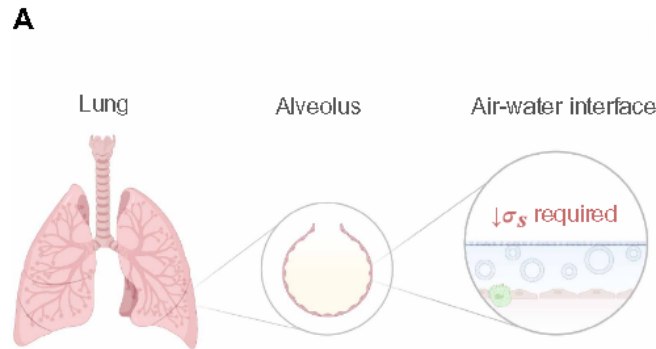
UNIVERSITY OF DELAWARE

Norman Wagner

QT trough

Quadrotrough: *In situ* Lung surfactant microstructure

SCIENCE ADVANCES | RESEARCH ARTICLE



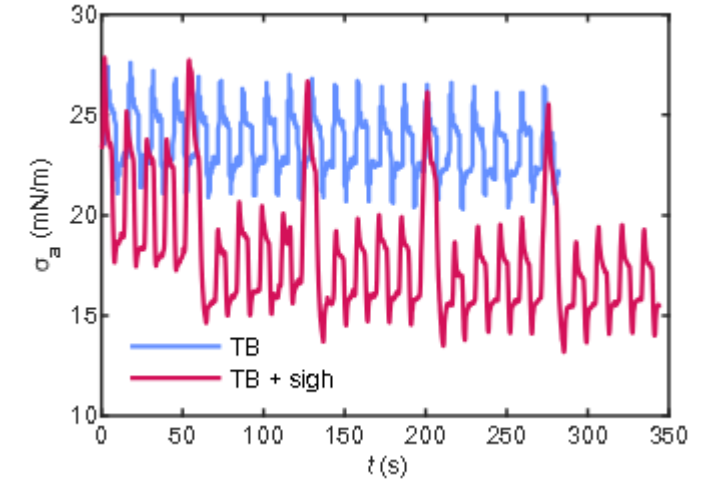
TB
 $t < 80$ min

TB + sigh
 $t < 80$ min

TB
 $t > 80$ min

TB + sigh
 $t > 80$ min

Mimicking breathing cycles



Novaes-Silva *et al.*, *Soft Matter* **21** 7963 (2025).
 Novaes-Silva *et al.*, *Sci. Adv.* **11** eadx6034 (2025).

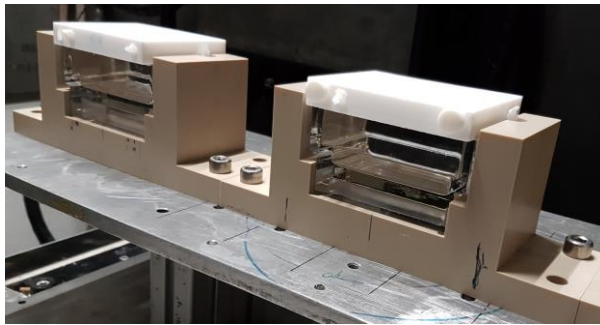
Example III: Bulk oil/water interface

Why liquid/liquid? Why FIGARO?

Liquid/liquid interface important for:

- Stabilisation of emulsion
- Mixed surfactants and cold water cleaning
- Transport properties of cell membrane
- Proteins (and surfactants) at Oil / Water
- Diverse range of colloids

Current design:



Drawbacks of current design:

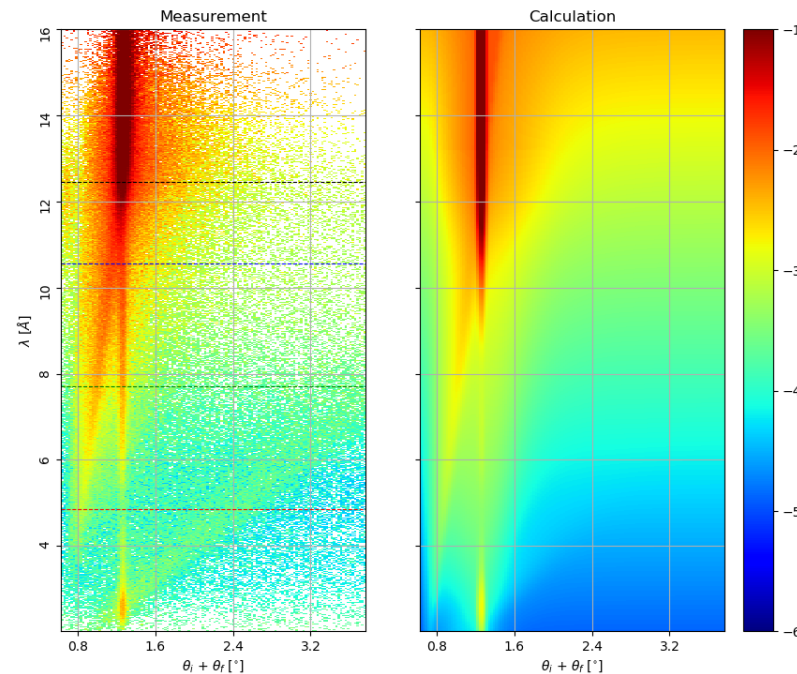
- Designed only for liquid/liquid interface, hence solid/liquid interface not (easily) accessible.
- Not machined, so edges are not sharp -> Difficult alignment.

FIGARO is very flexible, can reflect up or down,

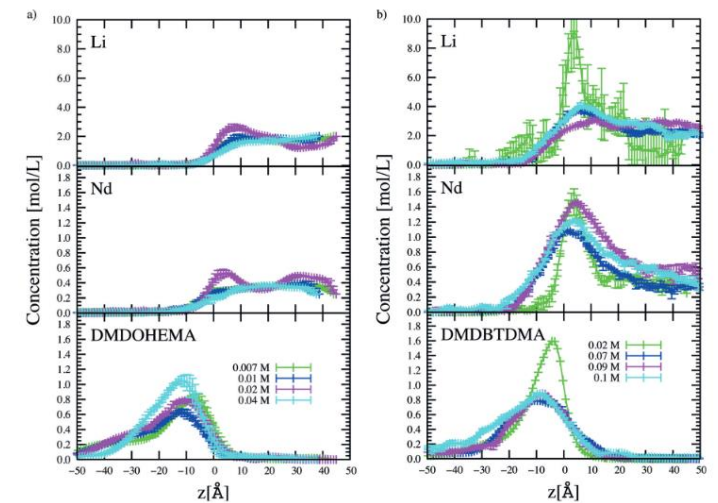
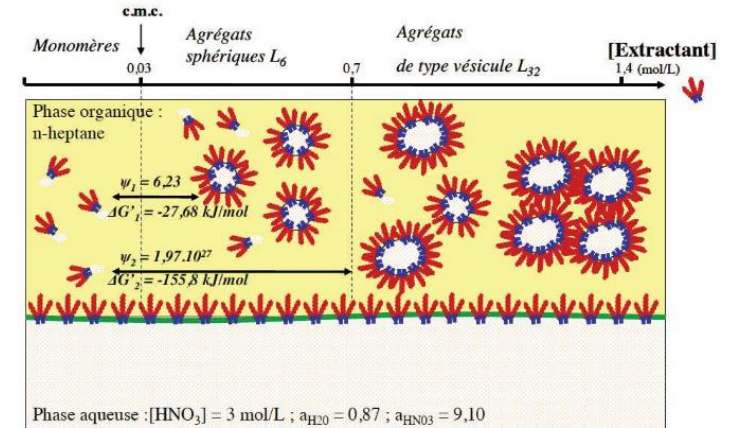
High flux, 2D detector

Off-specular scattering of lipid multilayer

At the oil/water interface:



Liquid/liquid interface in solvent extraction:



Example IV: NPs at the silicon-water and air-water interface (FIGARO (NR+OSS) and D22 (GISANS))

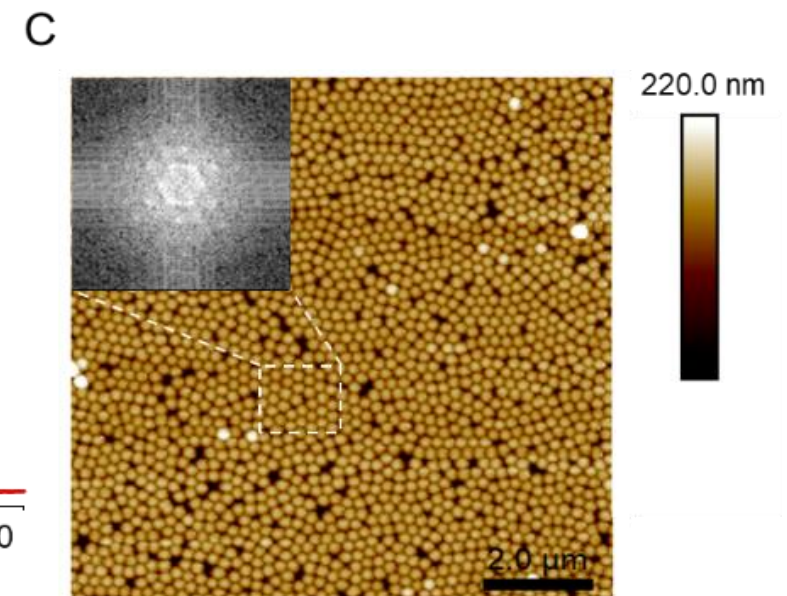
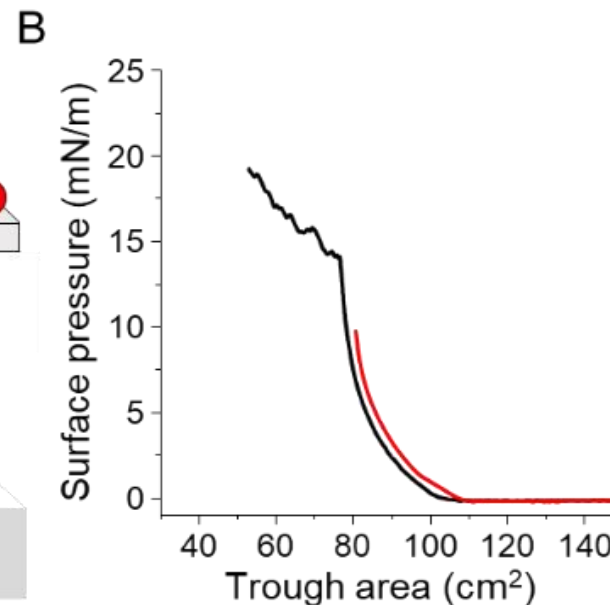
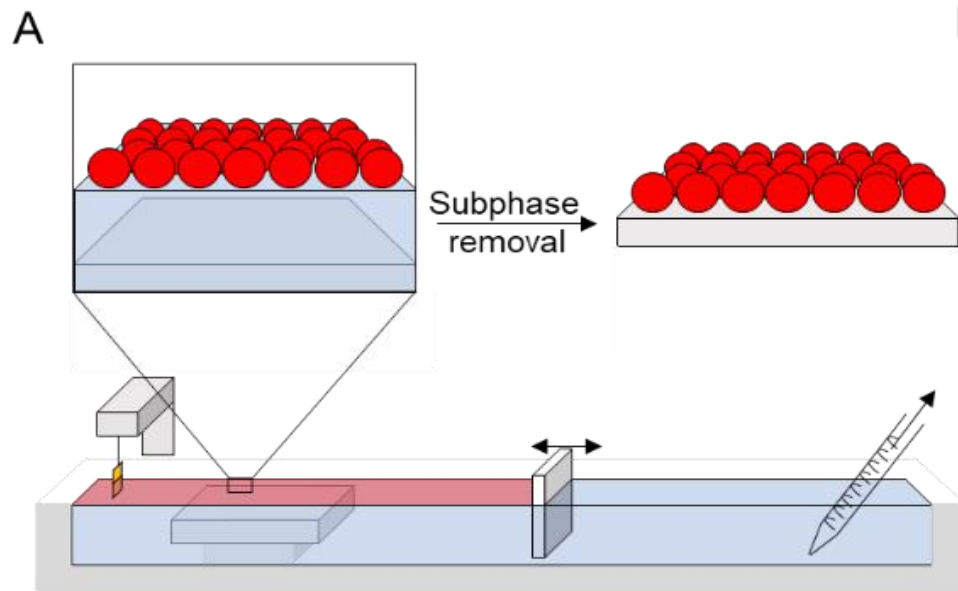


UPPSALA
UNIVERSITET



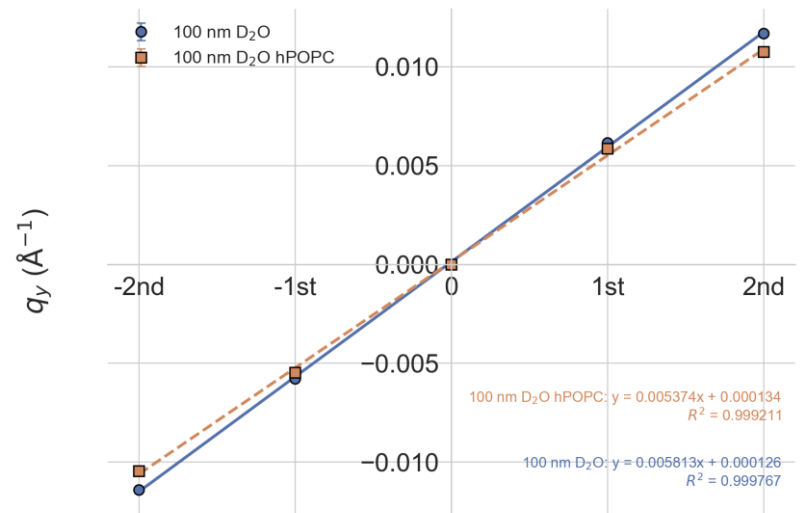
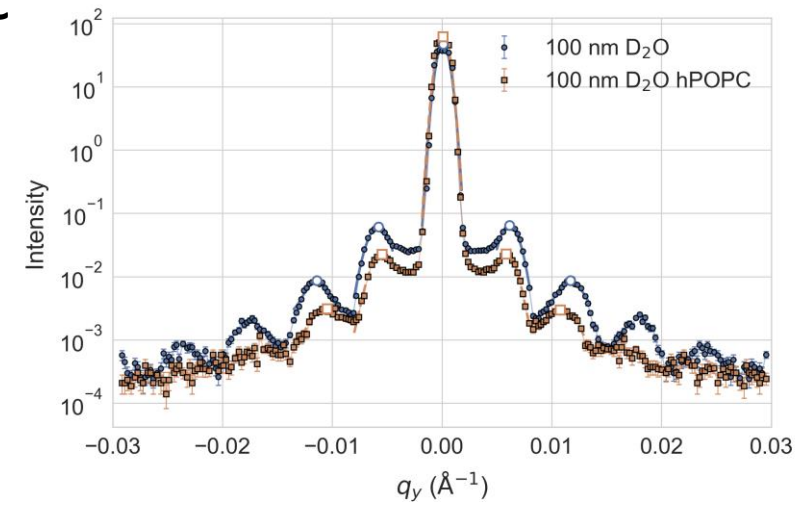
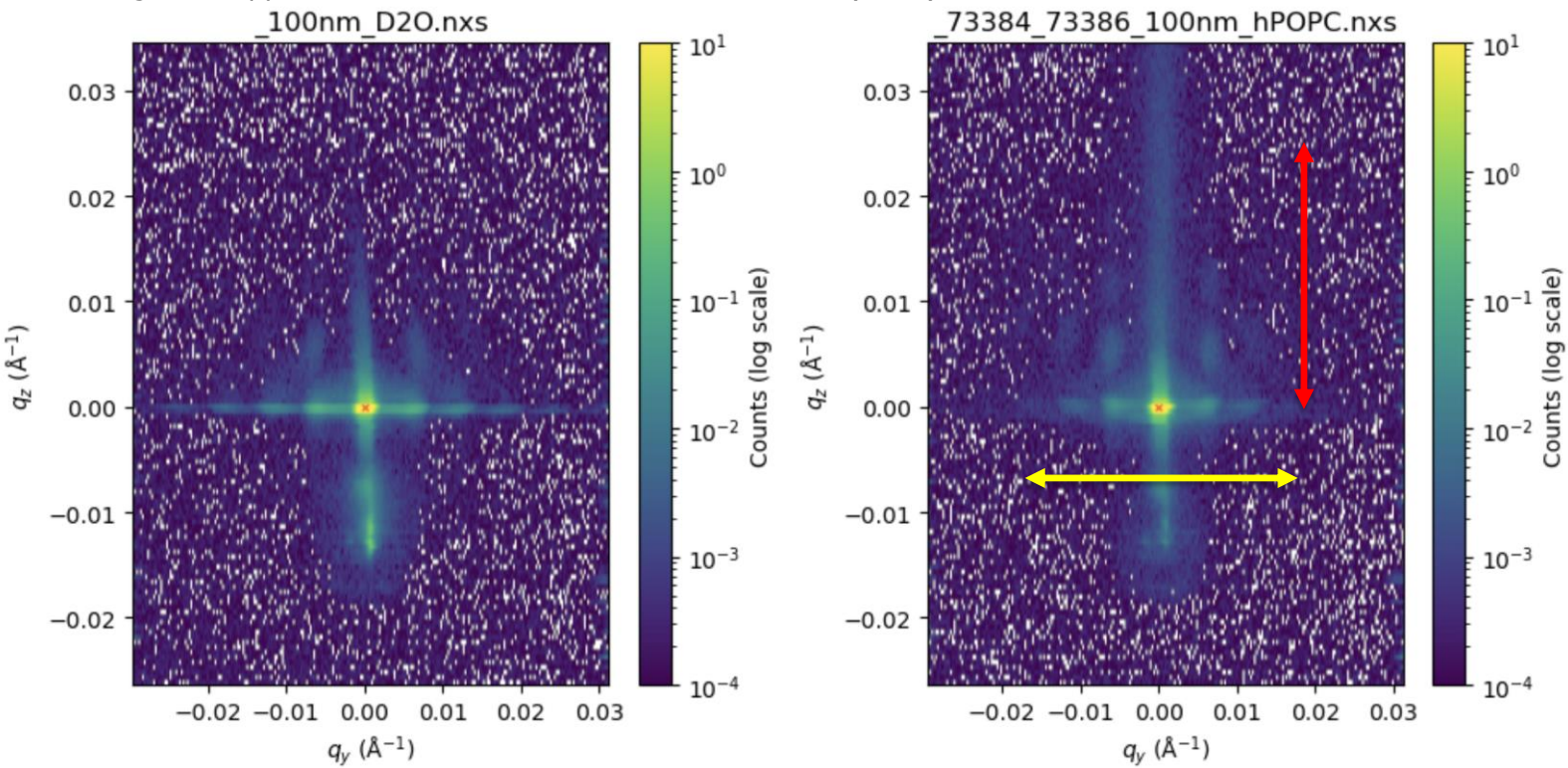
Nico Paracini, Max Wolff, Marite Cardenas

neutrons



100 nm – from D₂O to D₂O+hPOPC

N. Paracini, P. Gutfreund *et al.* - Structural Characterization of Nanoparticle-Supported Lipid Bilayer Arrays by Grazing Incidence X-ray and Neutron Scattering, *ACS Applied Materials & Interfaces* **15** 3772-3780 (2023).



Addition of lipids on 100 nm causes shift in peak position compatible with bilayer formation

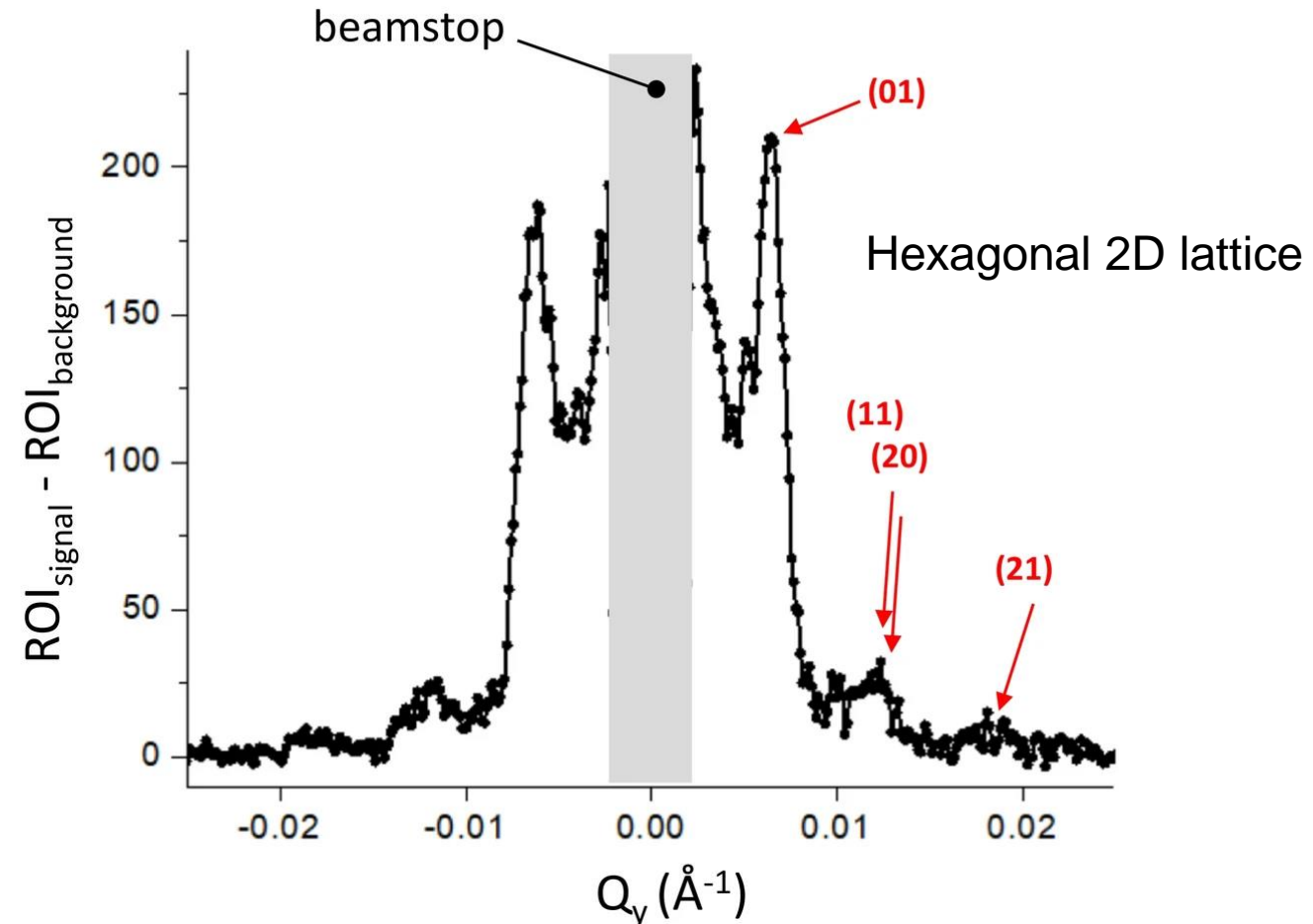
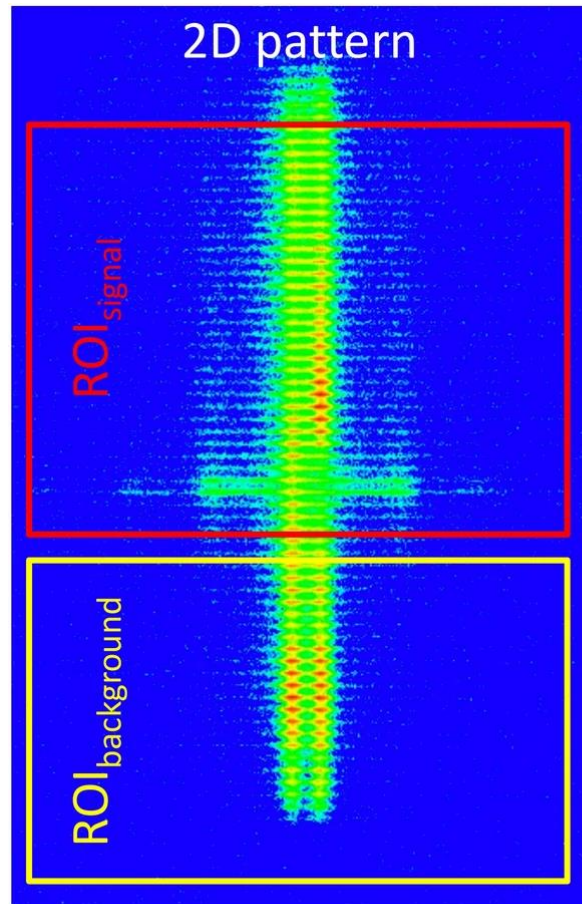
Significant loss of intensity in q_y after adding the lipids
 Increased intensity along q_z

$\Delta d \text{ D}_2\text{O} = 1080.8 \text{ \AA}$ Reflection order
 $\Delta d \text{ D}_2\text{O hPOPC: } d = 1169.2 \text{ \AA}$
 difference = 88.3 Bilayer formation

NR shows no bilayer formation on flat silica

NPs at air-water interface

Pseudo-GISANS on S-ADAM 100 nm NPs:



Vorobiev, A. et al., *Scientific Reports* (2021) 11, 17786.

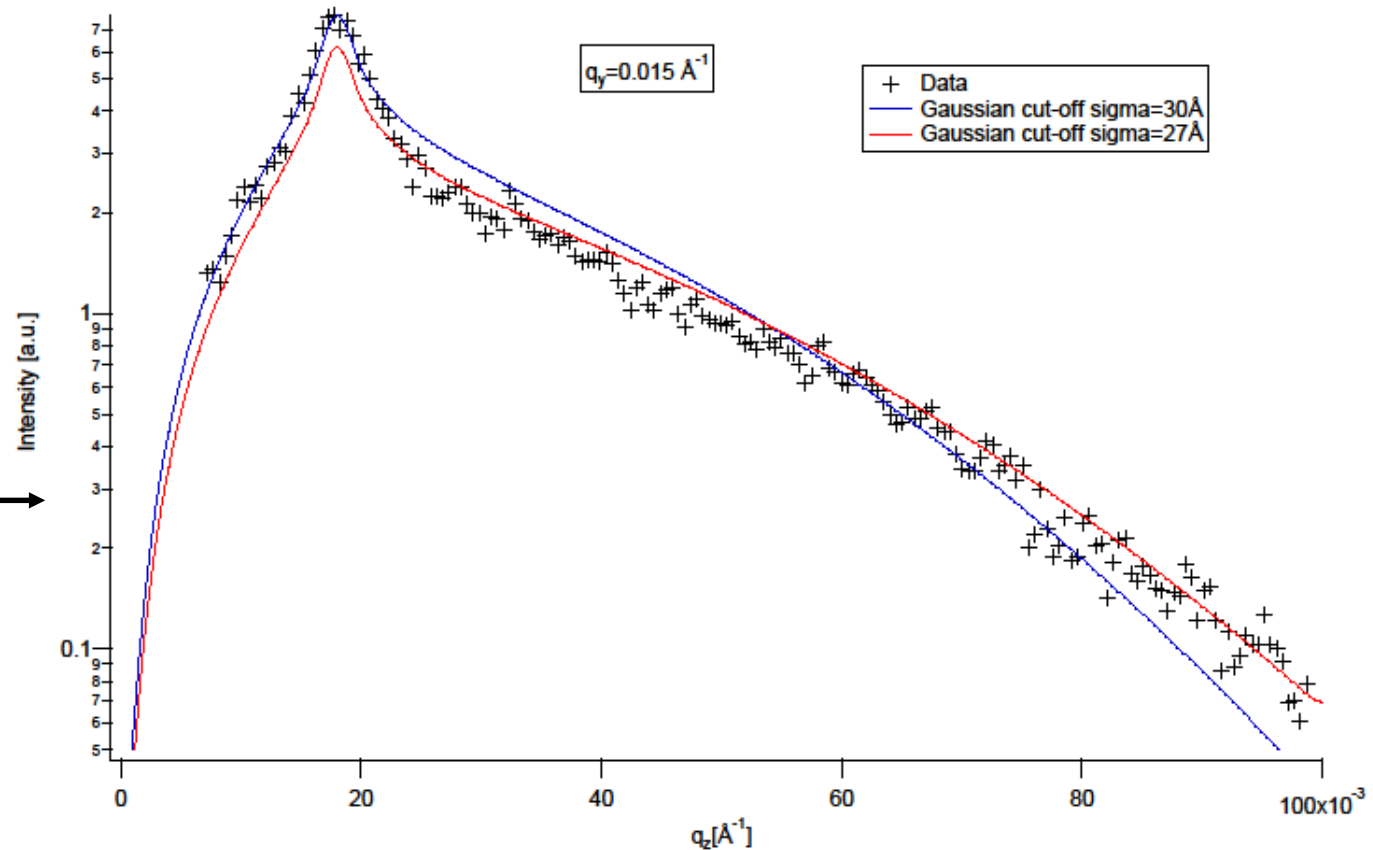
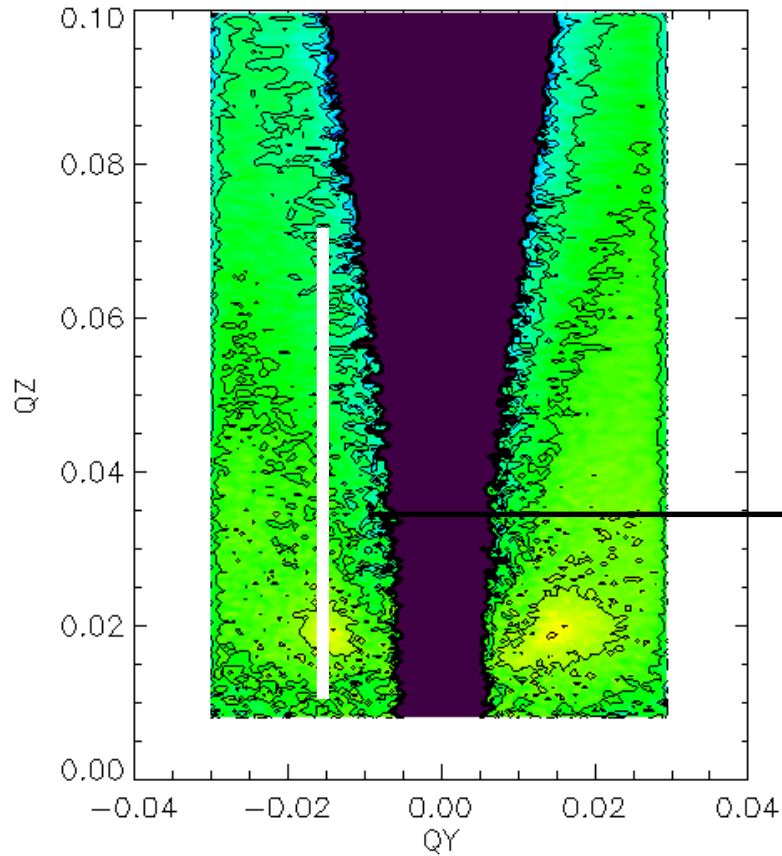


Pseudo- GISANS allows to extract the mean in-plane distance/lattice and/or size between NPs.

NPs at air-water interface

GISANS on FIGARO 30 nm NPs
With C-TAB:

Mean in-plane distance between NPs: 41 nm
Part of NP particle in air: 10 nm



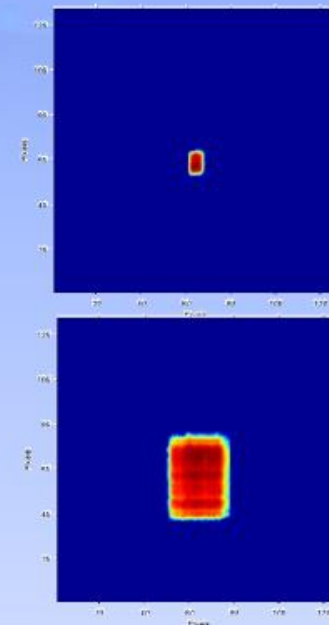
→ GISANS allows to extract the mean in-plane and out-of-plane size.

Small-Angle Neutron Scattering:

Resolution effects

- Beam Divergence, $\delta\theta$, determined by collimation distance and source aperture size

- Try to keep within the 'pin-hole' approximation for the sample size
- Beam 'size' on the detector
- Most important for detector pixels close to the beam centre



- Wavelength spread, $\delta\lambda/\lambda$:

- Typically 10% from a velocity selector
- $\delta\lambda$ leads to a radial ($|q|$) smearing of data



- Most important for scattering at higher angles
..... and could be relaxed further under some conditions to gain flux
..... but need also an option for higher resolution for some highly ordered systems

Microgels at the air/liquid interface

Fig. 2: Structure of 5 mol% cross-linked microgels at liquid interfaces.

